8-11-2015

Brain Connectivity changes after Stroke and Rehabilitation

Sahil Bajaj

BRAIN CONNECTIVITY CHANGES AFTER STROKE AND REHABILITATION

by

SAHIL BAJAJ

Under the Direction of Mukesh Dhamala, PhD and Andrew J. Butler, PhD

ABSTRACT

Several cortical and subcortical areas of brain interact coherently during various tasks such as motor-imagery (MI) and motor-execution (ME) and even during resting-state (RS). How these interactions are affected following stroke and how the functional organization is regained from rehabilitative treatments as people begin to recover have not been systematically studied. Role of primary motor area during MI task and how this differs during ME task are still questions of interest.

To answer such questions, we recorded functional magnetic resonance imaging (fMRI) signals from 30 participants: 17 young healthy controls and 13 aged stroke survivors following stroke and following rehabilitation - either mental practice (MP) or combined session of mental practice and physical therapy (MP + PT). All the participants performed RS task whereas stroke survivors performed MI and ME tasks as well. We investigated the activity of motor network consisting of the left primary motor area (LM1), the right primary motor area (RM1), the left pre-motor cortex

(LPMC), the right pre-motor cortex (RPMC) and the midline supplementary motor area (SMA). In this dissertation, first, we report that during RS the causal information flow (i) between the regions was reduced significantly following stroke (ii) did not increase significantly after MP alone and (iii) among the regions after MP+PT increased significantly towards the causal flow values for young able-bodied people. Second, we found that there was suppressive influence of SMA on M1 during MI task where as the influence was unrestricted during ME task. We reported that following intervention the connection between PMC and M1 was stronger during MI task whereas along with connection from PMC to M1, SMA to M1 also dominated during ME task. Behavioral results showed significant improvement in sensation and motor scores and significant correlation between differences in Fugl-Meyer Assessment (FMA) scores and differences in causal flow values as well differences in endogenous connectivity measures before and after intervention. We conclude that the spectra of causal information flow can be used as a reliable biomarker for evaluating rehabilitation in stroke survivors. These studies deepen our understanding of motor network activity during the recovery of motor behaviors in stroke. Understanding the stroke specific effective connectivity may be clinically beneficial in identifying effective treatments to maximize functional recovery in stroke survivors.

INDEX WORDS: Functional magnetic resonance imaging, Spectral Granger causality, Dynamical causal modeling, Stroke recovery, Rehabilitation, Motor network

BRAIN CONNECTIVITY CHANGES AFTER STROKE AND REHABILITATION

by

SAHIL BAJAJ

A Dissertation Submitted in Partial Fulfillment of the Requirements for the Degree of

Doctor of Philosophy

in the College of Arts and Sciences

Georgia State University

2015

BRAIN CONNECTIVITY CHANGES AFTER STROKE AND REHABILITATION

by

SAHIL BAJAJ

Committee Chair: Mukesh Dhamala

Andrew J. Butler

Committee: Vadym Apalkov

Igor Belykh

Brian D. Thoms

Electronic Version Approved:

Office of Graduate Studies

College of Arts and Sciences

Georgia State University

August 2015

DEDICATION

To my loving parents and my first teachers, Sham Lal and Darshana Bajaj

And

My loving wife Ramandeep

ACKNOWLEDGEMENTS

First and foremost, a big thanks to my principal supervisor, Dr. Mukesh Dhamala.

It would not have been possible to write this thesis without his endless help, support, and patience. His good advice, guidance and friendship have always been invaluable to me. I would like to acknowledge Dr. Andrew J. Butler for always being so generous and for his expertise and precious time. I am honored to have had the privilege of working with both of you- Dr. Dhamala and Dr. Butler. You consistently conveyed a spirit of adventure with regard to research.

I am very grateful to all the members of Neurophysics Research group and all my committee members. I would like to extend my thanks to Dr. Daniel Drake and Dr. Bhim M. Adhikari for their invaluable suggestions.

I also want to take this opportunity to thank my schoolteachers and mentors (especially, late Sh. Ranjit Sharma) for always inspiring me. A big thanks goes to my parents for their love and support throughout my life and for giving me strength to chase my dreams. Both of you are a great source of true inspiration- mom-dad. Also, I am very grateful to my elder brothers- Dr. Avinash Bajaj and Ashish Bajaj and their families who supported me in all my pursuits. My special thanks to my loving wife, Ramandeep, for all her devotion and love. Her sacrifices and encouragement throughout my career are truly undeniable.

Finally, I would like to thank all the wonderful people, friends and relatives who inspired and always supported me towards my graduate studies.

TABLE OF CONTENTS

LIST OF TABLES

LIST OF FIGURES

LIST OF ABBREVIATIONS

AB	able-bodied
BOLD	blood oxygenation level dependence
D	percent difference
DCM	dynamic causal modeling
df	small frequency interval
f	frequency
F	female
FA	flip angle
FMA	Fugl-Meyer Assessment
FMRI	functional magnetic resonance imaging
FOV	field of view
GC	Granger causality
IA	imagine affected
IU	imagine unaffected
*i*GC	integrated Granger causality
LFOs	low frequency oscillations
LM1	left primary motor area
LPMC	left premotor cortex
M	male
M	percent modulation
ME	motor execution
MI	motor imagination

MNI	Montreal Neurological Institute
MR	magnetic resonance
M1	primary motor area
MMSE	Mini-Mental State Exam
MP	mental practice
MP+PT	combination of mental practice and physical therapy
PA	pinch affected
PMC	premotor cortex
PT	physical therapy
PU	pinch unaffected
rs-fMRI	resting state- functional magnetic resonance imaging
RM1	right primary motor area
ROIs	regions of interest
RPMC	right premotor cortex
RS	resting state
S	spectral density matrix
SMA	supplementary motor area
SS	stroke survivors
TE	echo time
TR	repetition time
VOIs	volumes of interest
ΔFMA	difference between FMA scores before and after intervention
ΔGC	difference between GC values before and after intervention

1 INTRODUCTION

This dissertation mainly describes two studies on human brain motor network activity in stroke-survivors before and after intervention. First study describes reorganization and restoration of motor-network activity of stroke-survivors during resting-state [1]. Second study expands our understanding of motor network effective connectivity during motor-imagery and motor-execution tasks following stroke and intervention [2].

In chapter 2, we briefly describe the known causes behind stroke and available treatments. Chapter 3 includes a detailed description of the methodology, spectral version of Granger causality and dynamical causal modeling, used to explore connectivity patterns among regions involved in motor network. Chapter 4 describes how to identify an effective means of treatment for stroke-survivors to regain the strength of motor-behaviors and compares their strength with healthy volunteers. Chapter 5 pinpoints the role of primary motor area to differentiate the connectivity pattern discovered during motor-imagery and motor-execution tasks. Chapter 6 summarizes the main conclusions of both the studies.

This dissertation is based upon the following two peer-reviewed publications:

- **Bajaj, S.**, Butler, A.J., Drake, D., Dhamala, M. (2015) Functional organization and restoration of the brain motor-execution network after stroke and rehabilitation. *Frontiers in Human Neuroscience* 9:173.
- **Bajaj, S.**, Butler, A.J., Drake, D., Dhamala, M. (2015) Brain effective connectivity during motor-imagery and execution following stroke and rehabilitation. *NeuroImage: Clinical* 8: 572-582.

Other relevant peer-reviewed publications that are not included in this dissertation are following:

- **Bajaj, S.,** Adhikari, B. M., Dhamala, M. (in preparation). Bridging the gap: Dynamical causal modeling versus Granger causality analysis during resting state fMRI.
- **Bajaj, S.,** Drake, D., Butler, A.J., Dhamala, M. (2014). Oscillatory motor network activity during rest and movement: an fNIRS study. *Frontiers in Systems Neuroscience* 8 (13).
- **Bajaj, S.,** Lamichhane, B., Adhikari, B.M., Dhamala, M. (2013). Amygdala mediated connectivity in perceptual decision-making of emotional facial expressions. *Brain Connectivity* 3, 386–397.
- **Bajaj, S.,** Adhikari, B. M., Dhamala, M. (2013). Higher frequency network activity flow predicts lower frequency node activity in intrinsic low-frequency BOLD fluctuations. *PLoS ONE* 8: e64466.

2 STROKE AND REHABILITATIVE TREATMENTS

2.1 Stroke

The brain is known to be a self-organizing dynamical system with ongoing neural oscillations coherent across anatomically distinct and efficiently connected brain regions [3]. These coherent oscillations are the backbone of whole-brain functional connectivity networks such as default mode network and motor network [4]. Stroke often leads to functional imbalance within the motor network due to insufficient or no blood flow to part of the brain or due to direct tissue loss. This functional imbalance within the motor system following stroke [5-8] can be due to the damage in the white axonal tracts connecting brain motor areas [9,10]. In about 80% cases, this happens due to clotting of blood, known as ‘ischemic stroke’ and in the rest, this happens due to bursting of weak blood vessels, known as ‘hemorrhagic stroke’.

Main causes behind ischemic stroke include (i) building up of atheroma, abnormal small fatty lumps, along the walls of an artery (ii) infections that narrow blood vessels leading to brain and (iii) sudden drop in blood pressure. About 10% of strokes occur in young adults (under the age of 45) and the main causes included hypertension, tumors, migraine, consumption of alcohol and other drugs such as cocaine and amphetamines, which may also narrow the blood vessels. Sometimes breaking off atheroma also causes blockage of blood when it flows with the blood and stops in smaller arteries. On the other hand, hemorrhagic stroke mainly occurs when weak blood vessels rupture due to (i) abnormal accumulation of blood (ii) head injury (iii) brain tumors and (iv) decrease in the levels of blood platelets due to bleeding disorders. There is another kind of stroke, known as 'transient ischemic attack' or TIA, also called 'mini-stroke' or 'warning stroke'. It has same origins as that of ischemic stroke but it lasts only few minutes (less than 5 minutes) and doesn't cause permanent disability. About one-third of people who have TIA, suffer from stroke within a year.

Stroke may result into temporary or permanent physical disability among stroke survivors. Every year, more than 750,000 people suffer from stroke and about 80% of them experience trouble in moving their body parts. General statistics by National stroke association show 10% of stroke survivors recover almost completely whereas 15% die shortly after stroke and the rest either recover with impairments or require special long-term care. These statistics are a mere reflection of the lack of our understanding of the extent of brain function damage due to stroke and recovery following rehabilitative treatments. Functional neuroimaging studies on healthy volunteers have shown that several cortical areas of the human brain motor system interact coherently in the low frequency range (< 0.1 Hz), even in the absence of explicit stimulation or tasks. Following stroke, these cortical interactions are functionally disturbed. How these interactions are affected and how the

functional organization is regained from rehabilitative treatments as people begin to recover motor behaviors has not been systematically studied.

2.2 Rehabilitative treatments

Goal of rehabilitative treatments is to help the stroke survivors in learning the lost skills e.g. coordinating their hand movements in order to do a task, when some part of their brain is affected or completely damaged. Recently, several new rehabilitative interventions have been introduced. Some stroke survivors use multiple interventions or combination of few interventions and for some duration of intervention is longer compared to others, depending on their recovery, severity of their symptoms and how they respond to the treatments.

Rehabilitative treatments mainly include- (i) dynamic splinting which helps the stroke survivors to straighten their wrists and fingers (ii) electrical muscle simulation (EMS) which helps in moving weak limb by using electric impulses delivered directly to skin using electrodes (iii) robotic therapy devices-which guide the users to execute repeated movements (iv) transcranial magnetic stimulation (TMS) which uses electromagnetic induction to induce weak currents and helps in causing activity in specific parts of brain and (v) mirror therapy- to make it appear as if stroke survivors are moving their affected arm, however, they actually look at the movement of their unaffected hand. These days' mental practice (MP) and physical therapy (PT) are two frequently used evidence-based clinical interventions to enhance upper limb motor function purportedly to improve motor movement, coordination and balance following stroke [11-13]. Motor imagery (MI) and motor execution (ME) are generally considered to be the most effective tasks in these treatments. MP or MI represent mental rehearsal of a motor action without any overt action; and has been shown to improve motor behaviors in people with neurologic disorders [14-16]. It involves the survivors imagining movement of their affected limb. It is the creation by the mind

referring to an experience, which can be auditory, visual, tactile or kinesthetic representing movement. Likewise various forms of PT have been shown to be effective in ameliorating motor weakness following stroke [17,18]. It consists of more or less intensive affected limb exercise, restricting the unaffected arm over a long period of time.

In this thesis, we report findings from 17 young able-bodied participants and 13-aged stroke survivors. Six stroke participants were randomized to "mentally practice" (MP) a series of upper limb functional motor tasks for four hours per day (8-30 minute sessions), with the guidance of an audio tape, for a total of 60 hours over three weeks. Rest seven participants were randomized to undergo MP+ physical therapy (PT). The MP+PT group underwent 15 days (4 hours per day) of intensive one-on-one therapy, consisting of listening to the same MP tape for 60 minutes per day plus 3 hours of physical therapy per day. Identical tapes were given to all participants and the six mental practice tasks did not change, but small details of the mental practice scenarios such as the type of drink or color/type of telephone one reached for were altered to enhance motivation and lessen boredom. All sessions had identical contact durations and were monitored by a licensed rehabilitation specialist. The investigators were blind to group assignment. Following the three-week "training" period all participants underwent a second testing session recording both clinical and physiologic measures.

3 BRAIN CONNECTIVITY MEASURES

3.1 Directed functional and effective connectivity measures

Over the last few years, many techniques have been proposed describing how different brain areas interact with each other under different tasks and conditions. Several neuroimaging studies are available describing the internal mechanisms of brain under rest and task, explaining merits and

demerits of different connectivity approaches. Recently, the concepts of directed functional connectivity and effective connectivity have become very prominent in the field of computational neuroscience [19]. Directed functional connectivity approaches, e.g. Granger causality (GC) [20], assesses the cyclic functional association, among different brain areas. This approach is exploratory enough and uses the idea of predictability and statistical dependencies to establish causal relations. On the other hand, effective connectivity approaches, e.g. dynamic causal modeling (DCM) [21], assumes brain as a dynamic system and makes inferences about the influence of one neural system over the other. This approach is based on strong theoretical assumptions and specifies different hypothesis in terms of different models.

GC and DCM are the two most common and predominant techniques for exploring directionality among brain regions using electro/magneto encephalography (EEG/MEG) and fMRI data. However, both have been a topic of debate from quite a long time because of their own merits and demerits over each other. GC is mostly implemented via linear vector autoregressive (VAR) modeling. It has capability of having time and frequency components simultaneously at which different areas interact with each other. It can also be formulated in a way to evaluate exchange of causal information among multivariate sets of responses.

Applications of GC have also been mentioned as controversial recently [19,22] and had been a topic of debate in recent years. Some of the studies showed empirical and theoretical concerns regarding its applications for fMRI data [22-24]. Especially, it was thought that GC could be problematic and miss-lead the causal influences because of variability in shape and latency of hemodynamics response functions (HRFs) within brain and subject-wise as well [25-27]. FMRI demonstrates that hemodynamic response function is not identical and varies over the brain regions and individuals [25], violating temporal precedence assumptions made in GC. However, it is a very

well accepted measure used in analysis of electrophysiological time-series because of zero temporal-lag between the responses [28,29]. Although, Seth and colleagues in 2013 confirmed through a set of simulations that GC is invariant to convolution of hemodynamic response function but down-sampling the data to a variety of frequency severely interrupts the inferences made from GC [30]. Also, a simulation study done by Deshpande and his colleagues in 2010 found that GC was flexible enough to compensate hemodynamic variability [31]. Bressler and Seth in 2010 very well explained the applicability of GC to fMRI- showing GC as a well established methodology to estimate causal statistical influences directly from data [32]. They stated that HRFs are invariable across the conditions and de-convolution of fMRI BOLD signals can be used to measure the neural processes [26,33]. In addition to that, not only neural activity but various other factors like slice timing differences, baseline cerebral blood flow, baseline hematocrit, hemo-dilution, alcoholic/lipid intakes, different respiration rates across individuals are also responsible for HRFs variability [31,34-36]. Apart from that, it was also found that lower sampling rates could misinterpret fMRI GC [30,31]. In the near future, because of advancement in technology, it seems that the concerns associated with lower sampling rate won't remain a major problem [37]. Wen and colleagues in 2013 addressed the effect of various factors like (a) latency differences in HRF across different brain areas (b) low-sampling rates and (c) noise by linking fMRI GC and neural GC using simulated data [38]. For TR = 2 s and signal to noise ratio (SNR) = 5 (20% noise), they found a significant positive linear relationship ($r = 0.96$, $p = 0$) between the two in case of unidirectional coupling where as there was no correlation found in reverse coupling. Correlation was improved at higher sampling rates. This study in agreement with various other studies clarified that the convolution of HRF had no negative impact on GC calculations where as severe down sampling and presence of noise beyond a certain limit can worsen the GC interpretations [38-40].

On the other side, DCM relies on probabilistic graphical models, which are specified in terms of priors on the coupling parameters. It assumes that causal interactions among brain areas are mediated by hidden neuronal dynamics, specified in terms of non-linear differential equations in continuous time. Parameters of these equations reflect the connection strength, which are estimated using Bayesian techniques [21,41]. DCM doesn't encounter the controversies raised due to non-identical nature of hemodynamic response function because it directly models the hidden state variables, which cause observed data. It was found that DCMs, which involved hidden state variables, outperformed the DCMs, which were based on observations only [42].

Besides the fact that both GC and DCM are based on different facts and ideas, yet it was suggested that both are complementary to each other and may be converging at some point [43,44]. In the present thesis, we have used both of these approaches: GC for resting-state fMRI data and DCM task based fMRI data.

3.2 Spectral Granger causality measures

Spectral Granger causality measures are a subset of spectral interdependency measures [45]. Spectral interdependency measures are a means of statistically quantifying the inter-relationship between oscillatory processes; say 1 and 2, as a function of frequency of oscillations. It consists of three sub-measures: total interdependence ($M_{1,2}$), one-way directional influence either from 1 to 2 ($M_{1\to2}$) or 2 to 1 ($M_{2\to1}$) and instantaneous causal flow ($M_{1.2}$) (Granger causality measures), which are derived from a spectral density matrix (S) and are related by equation:

$$M_{1,2} = M_{1\to2} + M_{2\to1} + M_{1.2} \tag{3.1}$$

Spectral matrix (S) is constructed parametrically from the time-series of oscillatory systems using autoregressive (AR) modeling [46]. Diagonal elements of the matrix, S represent node activity

in terms of spectral power as a function of frequency whereas directional influences i.e. Granger causality (GC) between 1 and 2 are given by:

$$M_{1\to 2}(f) = \ln \frac{S_{22}(f)}{\tilde{H}_{11}(f)\Sigma_{11}\tilde{H}^{*}_{11}(f)}$$
$$M_{2\to 1}(f) = \ln \frac{S_{11}(f)}{\tilde{H}_{22}(f)\Sigma_{22}\tilde{H}^{*}_{22}(f)}, \quad (3.2)$$

where $\tilde{H}_{11} = H_{11} + \frac{\Sigma_{12}}{\Sigma_{11}} H_{12}, \tilde{H}_{22} = H_{22} + \frac{\Sigma_{12}}{\Sigma_{22}} H_{21}$ represent new transfer function matrices for 1 and 2 respectively in terms of noise covariance matrix, Σ and transfer function matrix, H. These are estimated from the residual errors and the inverse of the Fourier transforms of the coefficients in autoregressive models respectively.

3.3 Dynamic causal modeling (DCM)

DCM is a hypothesis-based technique, which aims to describe how observed fMRI responses are generated using a set of differential equations. DCM allows incorporating known effects of interest and assessing task-dependent as well as tasking independent interactions among a set of regions through a set of matrices, known as endogenous connectivity matrix, A and modulatory matrix, B respectively [21,47]. It estimates three sets of parameters: (a) task independent endogenous connectivity (matrix A) among the regions representing influence without any external perturbation (b) task dependent modulation affects (matrix B) representing changes in endogenous connection strength due to external perturbations and (c) direct influence of an external input to a region (matrix C). The underlying idea behind this is that it considers the brain as a non-linear dynamic system where inputs are known along with experimental perturbations [21]. This makes it different and effective than other traditional approaches like Granger causality and structural

equation modeling which assume interactions being linear without considering external inputs and/or perturbations [48].

Basically, DCM inferences following two types of hypothesis based on question of interest:

3.3.1 Bayesian model selection (BMS) approach

BMS inferences on model structure as a whole, which is done by defining and constructing a model space. Model space is usually a set of models, where each model defines specific endogenous connections that are modulated by experimental perturbations. It is BMS procedure that identifies the model which best explains how the data is generated by calculating exceedance probability of each model [49,50]. Exceedance probability represents the degree of belief about a model having higher posterior probability than rest of the models [51].

Recently, the approach of BMS at the group level has been revised by Rigoux and his colleagues [52]. They extended BMS approach by introducing the 'Bayesian omnibus risk (BOR)' factor, which measures the statistical risk while performing group level BMS analysis. This approach compares the likelihood of apparent differences in model frequencies by comparing 'protected exceedance probabilities' of proposed models i.e. it quantifies if a model is more frequent than the other, above and beyond chance [52].

3.3.2 Bayesian model averaging (BMA) approach

For computational efficiency, BMA employs Occam's window and discards all the models with probability ratio < 0.05 compared to the optimal model [41,53]. It inferences on each connection of the optimal model found from BMS by averaging over all the optimal models from all the participants. Various statistical tests like t-test and ANOVA are used to find significant connection strength.

For group level inferences, BMS and BMA can be employed by either using fixed-effects (FFX) analysis or random-effects analysis (RFX) depending upon whether the effect of interest (model structure or parameters) is fixed or a random variable due to inter-subject variability (e.g. in case of patients) across the population [54].

4 FUNCTIONAL REORGANIZATION AND RESTORATION DURING REST FOLLOWING STROKE AND INTERVENTION

4.1 Introduction

Hemiparesis is one of the most common deficits observed following stroke [55]. It means slight weakness or paralysis on one side of the body. About 80% of people suffering from stroke suffer from weakness on one side of their bodies. Due to limited clinical data compared to healthy volunteers data, recovery and restorative brain mechanisms in stroke survivors are not clearly understood. Specifically, scientists have yet to identify specific node and network activities of damaged brains that are invoked and/or restored following rehabilitative treatments.

Mental practice (MP) and physical therapy (PT) are two evidence-based interventions currently used to improve motor movement, coordination and balance following stroke [11-13]. Here, we studied the brain network mechanism for motor function recovery as a result of: MP only and MP in combination with PT. We predicted that the interventions to improve motor performance in stroke survivors would change the characteristic features of the brain motor network activity in such a way as to have network commonalities with those of able-bodied healthy participants. The strength of oscillatory network activity would correlate with the improvement in motor behaviors independent of intervention or in either intervention. We tested this hypothesis by examining and comparing the brain motor network activity in people recovering from stroke following

interventions and healthy controls using intrinsic blood oxygenation kevel dependence (BOLD) functional magnetic resonance imaging (fMRI) measurements.

MP or motor imagery (MI) represents mental rehearsal of a motor action without any overt action; and has been shown to improve motor behaviors in people with neurologic disorders [14-16]. Likewise various forms of PT have been shown to be effective in ameliorating motor weakness following stroke [17,18]. Recent neuroimaging studies [56-59] have extensively studied the brain motor networks during resting-state (RS), motor imagery (MI) and motor execution (ME) and have shown that overlapping networks are engaged in these task conditions. Planning, initiation, guidance and coordination of voluntary movements could modulate functional connectivity in the motor networks in these tasks [60]. The motor network commonly includes: the primary motor area (M1), the pre-motor cortex (PMC) and the supplementary motor area (SMA) [59,61,62], which taken together play a dominant role in the development, specification and execution of action. Activity in these cortical areas during resting-state is thought to maintain a dynamic equilibrium but is modulated during a motor task by disturbing the balance and coordination of local mutation inhibition [60]. The primary motor area (M1) is one of the principle brain areas that generates and sends neuronal signals to control the execution of motor commands whereas secondary motor areas SMA and PMC are involved in motor planning, sending neuronal impulses to M1. Also, asymmetries in PMC play an important role in controlling interhemispheric interactions during bimanual motor task [63]. Anatomically, M1 is connected to SMA and PMC in the same as well as in the opposite hemisphere allowing bilateral activity during rest, unimanual and bimanual hand movements [3,64-66].

Low frequency oscillations (LFOs) (< 0.1 Hz) in BOLD fMRI signals reflect self-organizing dynamic behavior of the brain. Several cortical and subcortical regions, including motor regions M1, PMC and SMA, interact and coordinate within and across the hemispheres within the low

frequency (< 0.1 Hz) range during resting-state [4,67]. The origin and functional relevance of these oscillations have not been completely investigated [68-71]. An emerging, well-accepted notion is that these slow intrinsic fluctuations are believed to be associated with neural level excitability changes in cortical and subcortical networks [69,72,73] which provides neural substrates for the flexibility and variability in cognition and motor behaviors [74,75]. These slow coherent oscillations are the backbone of whole-brain functional connectivity networks such as default-mode networks [76,77] which are actively being investigated in basic and clinical neuroscience [78,79]. Despite tremendous progress in revealing these network patterns in resting-state and clinical cases, the spectral features of oscillatory network activity and their modulations in patients by task conditions or therapy are not completely understood.

In this study, using the spectral version of Granger causality techniques [46,80,81], we investigated how the oscillatory network activity in the low frequency band (<0.1 Hz) within the motor network reorganizes in aged stroke survivors compared to young able-bodied participants as these stroke survivors undergo two interventions, mental practice and combined mental practice and physical therapy. The motor network we studied included: the left M1 (LM1), the right M1 (RM1), the left PMC (LPMC), the right PMC (RPMC) and the SMA. Our prediction was that the strength of oscillatory network activity would correlate with the improvement in motor behaviors independent of intervention or in either intervention.

4.2 Materials and methods

4.2.1 Participants

We recorded resting-state fMRI data from a total of 30 adult participants (17 young able-bodied, 13 aged stroke survivors). All the participants were instructed to keep their eyes open

fixated on a cross in the center of a screen, relax and try not to fall asleep. Mean age of young able-bodied participants (all right-handed, 12 males) was 25.17±4.68 years and the mean age of aged stroke survivors (1 left-handed, 9 males) was 59.23±9.49 years.

Able-bodied participants: All the participants had no abnormal neurological history. None of them reported use of medication known to affect any neurological function. A written consent was obtained from each participant before the experiment. The experimental protocol had appropriate institutional review boards (IRB) approval.

Stroke survivors: To be included in the study, all stroke survivors had to be at least 18 years old, independent in standing, toilet transfer, and the ability to maintain balance for at least 2 min. with arm support. Upper extremity movement criteria included the ability to actively extend the affected wrist ≥20° and extend 2 fingers and thumb at least 10° with a motor activity log (MAL) score of less than 2.5 [82]. All of them survived their first stroke within 54 months prior to enrollment. Either MR imaging or computed tomography (CT) was used to confirm stroke and its location (Table 4.1). Stroke latency ranged from 1 to 54 months. Six of them had left hemiparesis resulting from infarct or hemorrhage located in the thalamus, basal ganglia, internal capsule, caudate, and/or precentral gyrus. The remaining volunteers had right hemiparesis due to infarctions of the middle cerebral, pontine or internal carotid arteries (Table 4.1) [8]. The Mini-Mental State Exam (MMSE) was used to assess cognitive aspects of mental function where a maximum score of 30 describes normal cognition function [83] (Table 4.1). This measure constituted two sets of questions - one set tested orientation, memory and attention whereas the second set tested the participant's ability to name, follow verbal and written commands, write a sentence spontaneously and copy a complex polygon. The Fugl-Meyer Motor Assessments (FMA) was used to assess sensation and motor functions. This included a total of 33 items including reflexes, volitional movement assessment, flexor synergy,

extension synergy, movement combining synergies, movement out of synergy, normal reflex assessment, wrist movement, hand movement, co-ordination and speed, each with a scale from 0 - 2 (0 for no performance, 1 for partial performance and 2 for complete performance) [84]. The total possible score was 66 where a score of nearly 33 represents moderate impairment of the affected upper limb.

Table 4.1 Clinical and demographic data.

Age (in years), sex, post stroke duration (in months), the Mini-Mental State Exam scores and stroke locations of the stroke group.

Participant	Age (years)	Sex	Post stroke (months)	MMSE	Stroke location
1	55	F	5	30	L thal. hem.
2	55	M	1	27	L basal ganglia
3	52	M	8	24	R cingulate gyrus infarct
4	74	F	9	30	R caudate infarct
5	65	F	7	28	L caudate infarct
6	54	M	11	27	R putamen hem.
7	50	M	5	30	R lacunar infarct (Globus pallidus)
8	69	F	8	28	R motor cortex infarct
9	64	M	54	28	R basal ganglia, thalamic hem.
10	42	M	5	30	R pontine infarct

11	55	M	7	28	L internal capsule
12	62	M	7	28	L thalamic hem.
13	73	M	5	28	L pontomedullary

M = male; F = female; MMSE = Mini-Mental State Exam.

4.2.2 Imaging

Each of the young able-bodied participants underwent one resting-state fMRI (rs-fMRI) scanning session. Imaging was performed using a 3-Tesla Siemens whole-body MRI scanner. Functional imaging was 7 minutes and 54 seconds long, and included a T2*- weighted echo planner imaging (EPI) sequence (echo time (TE)=40 ms; repetition time (TR)=2000 ms; flip angle=90 degrees; field of view (FOV)=24 cm, matrix=64x64; number of slices=33 and slice thickness=5 mm. High-resolution T1-weighted images were acquired for anatomical references using an MPRAGE sequence with an isotropic voxel size of 2 mm. Stroke participants underwent two rs-fMRI scanning sessions. The second session was executed following an intervention where stroke participants underwent either mental practice (MP) alone or mental practice combined with physical therapy (MP+PT). The gap between the sessions ranged from 14-51 days and had a different protocol than for young able-bodied participants. Their fMRI data was collected from a Siemens 3.0 T Magnetom Trio scanner (Siemens Medical Solutions, USA) and included TR/TE/FA=2350 ms/28 ms/90°, 130 time points (~5 min each), resolution=3x3x3 mm^3 and 35 axial slices.

4.2.3 Intervention details

The MP consisted of imagining four basic MI tasks using the affected or unaffected hand. For instance, participants were asked: (1) to imagine brushing or combing their hair, (2) to imagine picking up and bringing different types of fruit to their mouth, (3) to imagine extending their arm to

pick up a cup from a cabinet and place it on the counter and gently release it, and (4) to imagine cleaning the kitchen counter using a cloth.

The PT consisted of repetitive, task-oriented training of the more-impaired upper extremity for several hours a day (depending on the severity of the initial deficit). Task oriented training involved functionally based activities performed continuously for a period of 15-20 min. (e.g. writing in a journal). In successive periods of task training, the spatial requirement of the activity, or other parameters (such as duration), were changed to require more demanding control of limb segments for task completion. Feedback about overall performance was provided at the end of the 15-20 min. period. A large bank of tasks was created for use among participants. Frequent rest intervals were provided through the training session.

4.2.4 Data analysis

FMRI preprocessing: FMRI data were preprocessed by using SPM8 (Wellcome Trust Centre for Neuroimaging, London; http://www.fil.ion.ucl.ac.uk/spm/software/spm8/). The preprocessing steps involved slice time correction, realignment, normalization and smoothing. Motion correction to the first functional scan was performed within participant using a six-parameter rigid-body transformation. Six motion parameters (three translational and three rotational) were stored and used as nuisance covariates. Four able-bodied participants had either more than 2 mm of translation or more than 1.5° of rotation about the three axes and were excluded from the analysis. The mean of the motion-corrected images was then co-registered to the individual structural image using a 12-parameter affine transformation. The images were then spatially normalized to the Montreal Neurological Institute (MNI) template [85] by applying a 12-parameter affine transformation, followed by a nonlinear warping using basis functions [86]. Images were subsequently smoothed with

an 8-mm isotropic Gaussian kernel and band-pass-filtered (0.04-0.1 Hz) in the temporal domain.

Regions of interest: Regions of interest (ROIs) for motor-execution network were defined using seed-based correlation mapping procedure to assess functional connectivity among the regions. The left primary motor area (LM1) was selected as seed region with a 6 mm radius sphere centered at (-33.0, -19.8, 52.1) in the MNI coordinate system. Voxel-wise BOLD time series for all the regions were extracted by making masks using MARSBAR (http://marsbar.sourceforge.net/). The correlated regions to the LM1 were the right primary motor area (RM1) centered at (35.7, -18.1, 52.0), the left pre-motor cortex (LPMC) centered at (-34.3, -1.4, 55.8), the right pre-motor cortex (RPMC) centered at (35.1, 0.1, 54.9) and the midline supplementary motor area (SMA) centered at (0.0, -4.2, 64.7) as used in a previous study [8]. Previously, power spectra for data with TR>2 seconds showed peak at frequency less than 0.04 Hz due to motion parameters [71]. Therefore, in current analysis, we extracted data from all the regions, linearly detrended and band-pass filtered within the frequency range of 0.04 to 0.1 Hz.

4.2.5 Spectral Granger causality measures and significant tests

Using equation 3.2, Granger causality (GC) values were calculated among all the regions of interest and were integrated (*iGC*) over the frequency range from 0.04 Hz (f_1) to 0.1 Hz (f_2), say from region 1 to 2:

$$iGC_{1\to 2} = \frac{1}{f_2 - f_1}\int_{f_1}^{f_2} M_{1\to 2}(f)\,df \qquad (4.1)$$

Thresholds for significance level of Granger causality for each participant - able-bodied (AB), stroke survivors (SS), stroke survivors under treatments: mental practice (MP) and mental practice and physical therapy (MP+PT) were computed by random permutation method [87]. We considered

AB condition as reference level for SS to calculate percentage difference (D) in connectivity strength. SS was used as reference for MP and MP+PT to calculate percent modulation (M) after treatment of MP and MP+PT. This percent difference (D) and percent modulation (M) for SS and for MP and MP+PT respectively were calculated as follows [3]:

$$D = \frac{iGC_{SS} - iGC_{AB}}{iGC_{AB}} \times 100\% \quad (4.2)$$

$$M = \frac{iGC_{MP/MPPT} - iGC_{SS}}{iGC_{MP/MPPT}} \times 100\% \quad (4.3)$$

Here iGC_{SS}, iGC_{AB}, iGC_{MP} and iGC_{MPPT} represent integrated causal flow for stroke survivors (SS) (no treatment), young able-bodied (AB) participants, stroke survivors with treatment of mental practice (MP) only and stroke survivors with combined mental practice and physical therapy (MP+PT) respectively.

4.3 Results

4.3.1 Power and GC spectra

Power and GC spectra for all five ROIs (LM1, RM1, LPMC, RPMC and SMA) were computed for AB, SS, MP and MP+PT conditions. Average power spectra were computed from all subjects (Appendix A.1). Figure 4.1A shows group level comparison of power spectra of SMA for AB, SS, MP and MP+PT conditions. In all four conditions, for all the ROIs, the peaks for power were in the frequency band 0.06-0.08 Hz (Appendix A.1). Figure 4.1B shows a comparison of peak power of all ROIs for all conditions with standard error of mean. The peaks for GC spectra (Appendix A.2: A-G) were also found in the same frequency band 0.06-0.08 Hz. Dashed lines in the GC plots show a significant threshold ($p < 0.01$, sample size = 26) calculated from combined set of data for AB and SS.

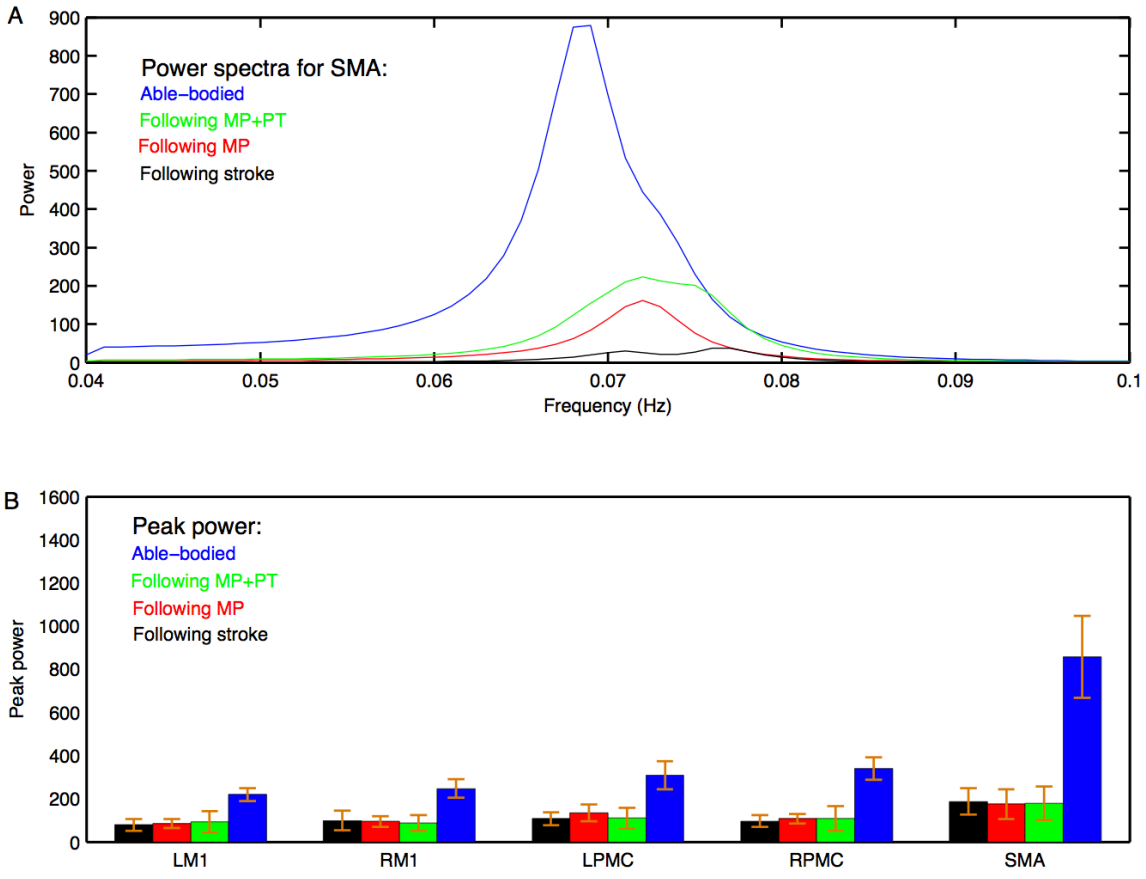

Figure 4.1 Power spectra and peak power.

(A) Peak of power spectra for SMA occurs within the frequency band 0.06 – 0.08 Hz for young able-bodied participants (blue colored plot), aged stroke survivors who underwent MP+PT (green colored plot), aged stroke survivors who underwent MP only (red colored plot) and for aged stroke survivors before intervention (black colored plot). (B) Peak power and the associated standard error of the mean for each ROI in each condition is shown.

4.3.2 Directed functional connectivity

Directed functional connectivity among five ROIs was computed for AB, SS, MP and MP+PT conditions. Figure 4.2A shows significant causal flow from SMA to LM1 for AB and SS

who underwent MP+PT. For AB, seven connections were found that had significant causal flow, including bidirectional causal flow between LM1 and SMA (Appendix A.2: A, D; blue line) and between RPMC and SMA (Appendix A.2: B, G; blue line). Other connections having significant causal flows were from RPMC to LM1 (Appendix A.2: C; blue line), SMA to RM1 (Appendix A.2: E; blue line) and SMA to LPMC (Appendix A.2: F; blue line). Compared to AB, the stroke survivors did not show significant causal flow (Appendix A.2: A-G; black lines). Compared to AB, stroke survivors who underwent MP only did not demonstrate any connections with significant causal flow (Appendix A.2: A-G, red line). On the other hand, stroke survivors who underwent combined MP + PT showed three connections: between LM1 and SMA (Appendix A.2: D; green line) and from SMA to LPMC (Appendix A.2: F; green line), with significant causal flows. Integrated causal flow for all seven connections was calculated by using equation 4.1 (Figure 4.2: B-H). Significant causal flows are marked with $*$ ($p < 0.01$, sample size = 26).

4.3.3 Connectivity modulations

We used equation 4.2 to compute percent difference (D) in connection strength for aged stroke-survivors (SS) with respect to young able-bodied (AB) people. We found that the strength of all the connections, which showed significant causal flow in AB, decreased and ranged from -21% to -97% (Figure 4.3: A-B). Connection between SMA and LM1 was the most negatively affected connection for aged stroke-survivors.

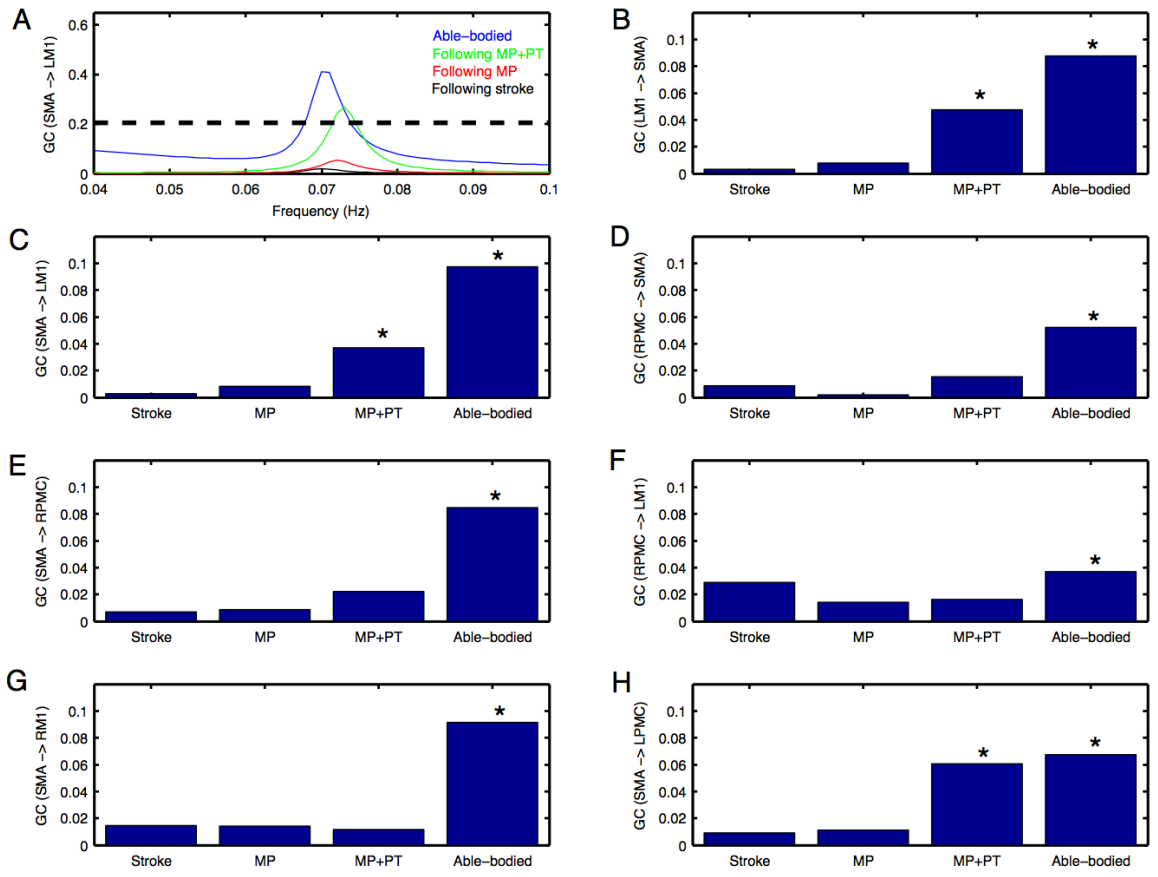

Figure 4.2 Granger causality (GC) spectra and integrated causal flow for young able bodied and aged stroke survivors before and after intervention.

Significant causal flow is obtained from (A) SMA to LM1 for young able-bodied participants (blue colored plot) and for aged stroke survivors who underwent MP+PT (green colored plot) whereas it is not significant before intervention (black colored plot) and when the aged stroke-survivors underwent MP only (red colored plot). Integrated causal flow for frequency band 0.04 – 0.1 Hz is calculated for all the seven significant connections (B-H). Here * represents significant causal flow values. Three connections: (B) LM1 to SMA (C) SMA to LM1 and (H) SMA to LPMC showed significant causal flow values for aged stroke survivors after MP+PT whereas none of the causal influences for aged stroke survivors are significant before and after MP treatments.

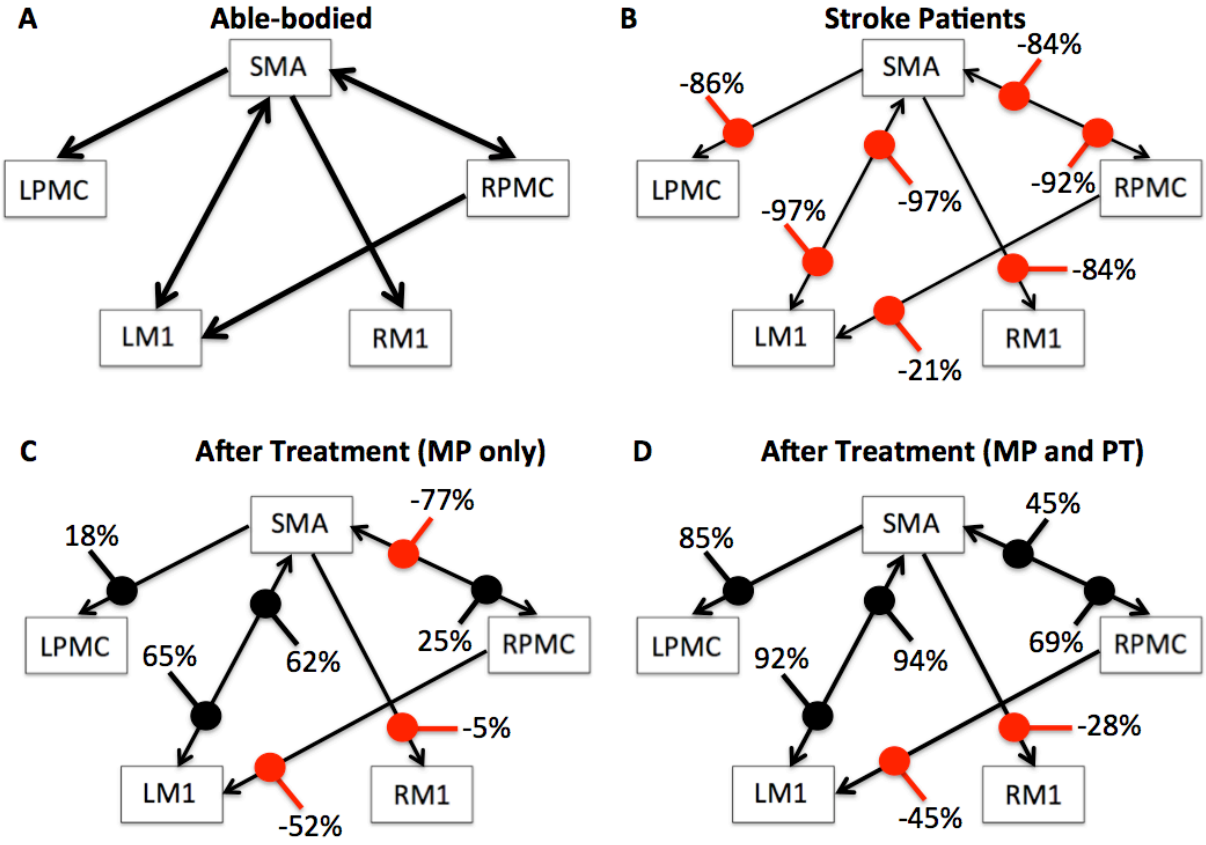

Figure 4.3 Percent difference and modulation.

Compared to (A) young able-bodied participants, percent decrease of the causal flow ranged from -21% to -97% for aged stroke patients as shown in (B), whereas compared to aged stroke patients, there was a percent modulation ranging from 18% to 65% for aged stroke patients who underwent MP as shown in (C) and from 45% to 94% for aged stroke patients who underwent MP+PT as shown in (D). Percent decrease and percent modulations are shown with red and black colored dots respectively.

We used equation 4.3 to compute the percent modulation (M) of aged stroke survivors, who had either MP or MP+PT treatment. We found that percent modulation for MP ranged from 18% to 65% (Figure 4.3C). The most affected connection found previously (between LM1 and SMA) was

modulated by 62%-65%. Three connections, from SMA to RM1, RPMC to LM1 and RPMC to SMA were negatively modulated by 5%, 52% and 77% respectively. We found that percent modulation for MP+PT ranged from 45% to 94% (Figure 4.3D). Here the most affective connections were modulated by 92%-94%, which is much higher than during MP only. Two connections, from SMA to RM1 and RPMC to LM1 were negatively modulated by 28% and 45% respectively.

We were also interested in finding whether or not the behavior of the network differs for AB, SS, MP and MP+PT groups and therefore we combined all seven significant connections in the network and performed two-sample (un-paired) t-test for AB vs. SS, SS vs. MP, SS vs. MP+PT and MP vs. MP+PT (Figure 4.4). We found that the network as a whole, consisting of seven significant connections, was significantly stronger for young able-bodied volunteers than for aged stroke-survivors ($p = 10^{-5}$, sample size = 13, denoted by $***$). We also found that there was no significant difference between the strength of networks when the aged stroke survivors had only performed MP ($p = 0.75$, denoted by NS) whereas the network became significantly stronger when the aged stroke survivors underwent combined, MP+PT ($p = 0.02$, denoted by $*$). We also found that the effect of MP+PT was significantly stronger than MP only ($p = 0.01$, denoted by $**$).

4.3.4 Brain and behavior correlation

FMA scores were recorded for all the aged stroke-survivors before and after the intervention. Using paired t-test, we found that FMA scores showed a trend towards significant increase when the participants underwent MP (sample size = 6; $p = 0.056$; paired t-test) (Figure 4.5A) whereas the scores increased significantly when the participants underwent MP+PT (sample size 7; $p= 0.033$; paired t-test) (Figure 4.5B).

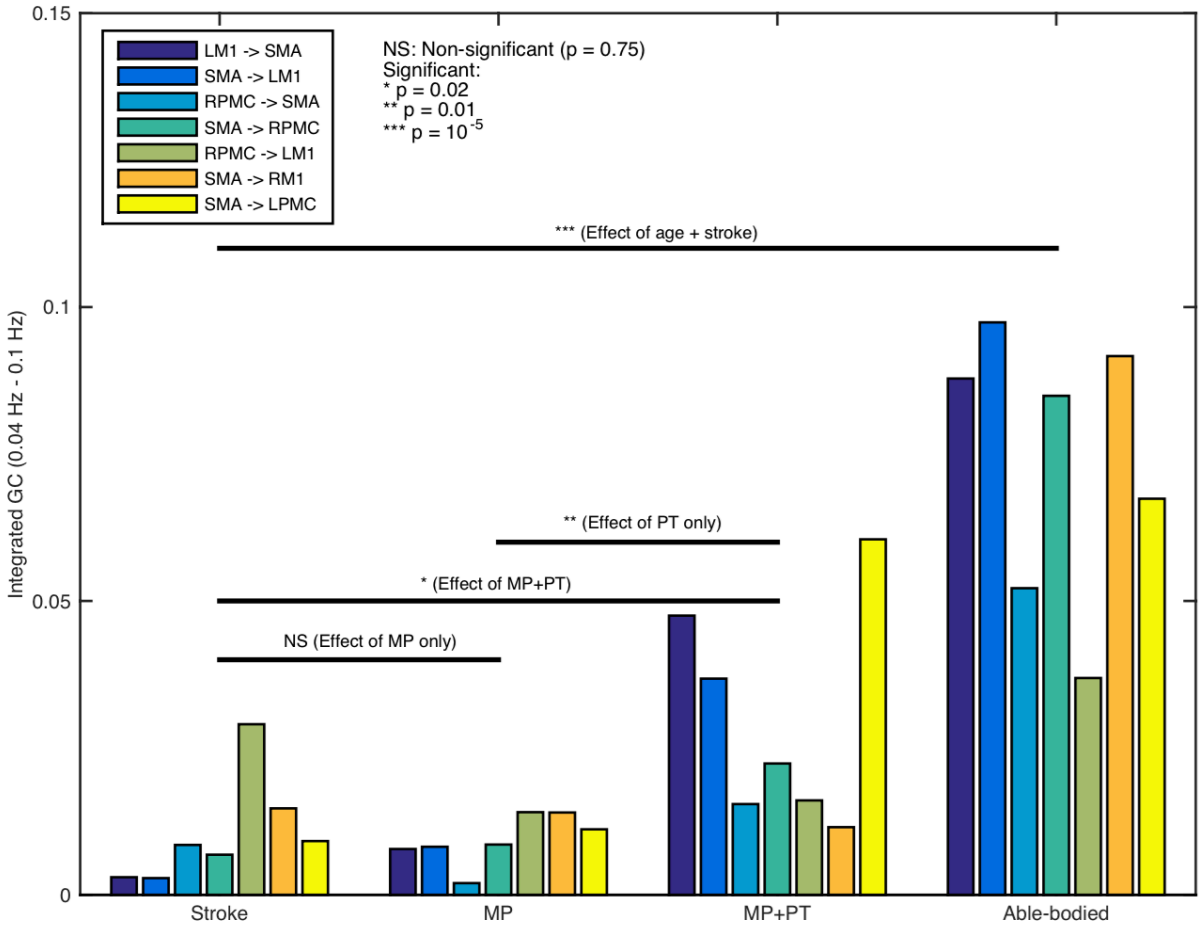

Figure 4.4 Network activity comparisons

Considering the causal influences for all significant connections, stronger network activity ($^{***}p = 10^{-5}$) was observed for young able-bodied participants than aged stroke-survivors. No significant difference between integrated causal flow values was found between aged stroke survivors before and after mental practice (MP) ($p = 0.75$) whereas network activity was significantly higher when they underwent combined session of mental practice and physical therapy (MP+PT) ($^{*}p = 0.02$). We also found that the network activity was significantly higher following MP+PT than following MP only ($^{**}p = 0.01$).

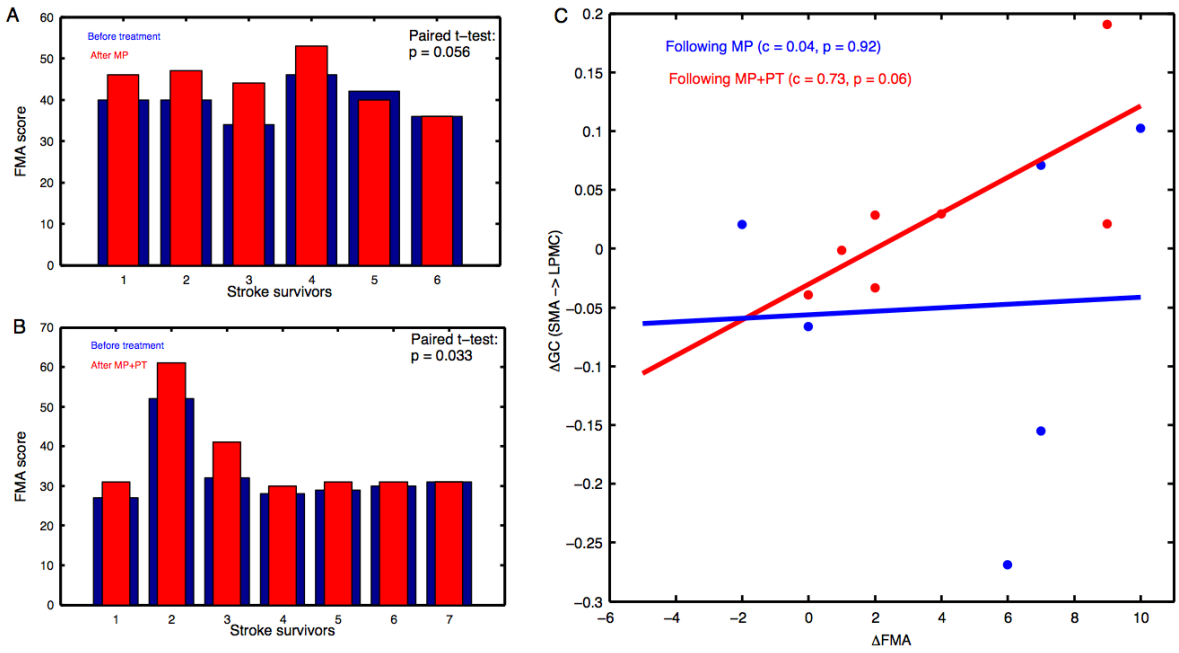

Figure 4.5 Brain and behavioral correlation

The Fugl-Meyer Motor Assessment (FMA) scores for aged stroke-survivors: (A) before intervention (blue bars) and after MP (red bars), and (B) before intervention (blue bars) and after MP+PT (red bars) are plotted. We also observed that for connection: (C) from SMA to LPMC, the correlation between differences in FMA scores (ΔFMA) and GC values (ΔGC) before and after MP+PT intervention showed a linear trend towards statistical significance but there was no trend observed for MP alone.

For the brain and behavior correlation, the behavioral FMA score difference (ΔFMA) and brain GC difference (ΔGC) showed a correlation trend for SMA to LPMC direction in case of MP+PT treatment, but there was no trend for MP alone (Figure 4.5C; Table 4.2).

Table 4.2 Brain and behavior scores.

Differences in FMA scores (ΔFMA) and GC values (ΔGC) before and after the intervention.

Participant	ΔFMA	ΔGC (following intervention-following stroke)		
		LM1 -> SMA	SMA –> LM1	SMA -> LPMC
Participants who underwent MP only: MP-stroke				
1	6	-0.36	-0.23	-0.26
2	7	0.00	0.08	0.07
3	10	-0.06	0.02	0.10
4	7	-0.01	-0.12	-0.15
5	-2	-0.01	0.00	0.02
6	0	0.01	-0.03	-0.06
Participants who underwent MP+PT: (MP+PT)-stroke				
7	4	0.04	0.00	0.02
8	9	0.1	0.10	0.02
9	9	-0.02	0.04	0.19
10	2	0.00	-0.17	0.02
11	2	0.09	0.15	-0.03
12	1	0.18	0.05	-0.00
13	0	0.03	-0.06	-0.03

ΔFMA = Difference between FMA scores following stroke and following intervention;
ΔGC = Difference between GC values following stroke and following intervention.

4.4 Discussion

In this study, we used the spectral GC approach on resting-state fMRI data of 30 participants to investigate the organization of motor-execution network for young able-bodied and aged stroke survivors along with substantial changes after the stroke survivors underwent mental practice alone or combined mental and physical therapy. We found that node and network activities were dominant in the frequency band 0.06 Hz - 0.08 Hz for all participants in all conditions. We found that node activity for each ROI was significantly higher in AB condition than SS condition but there was no significant difference between node activities for SS, MP and MP+PT conditions. There were bidirectional causal influences between LM1 and SMA, RPMC and SMA, RPMC and LM1, SMA and RM1, and SMA to LPMC for young able-bodied participants, but none of the directions were significant for aged stroke survivors even when they underwent a session of MP. Some of the connections, for example between LM1 and SMA and from SMA to LPMC, showed significant causal flow when aged stroke survivors underwent combined session of MP and PT (MP+PT). Percent decrease in connection strength reflected by causal flow for aged stroke survivors compared to young able-bodied ranged from -21% to -97% whereas the percent modulation for aged stroke survivors with MP and MP+PT compared to those individuals receiving no treatment ranged between 18% to 65% and 45% to 94% respectively. Furthermore, as predicted young able-bodied participants demonstrated significantly stronger causal influence than aged stroke survivors. There was no significant difference in causality before and after the MP treatment in aged stroke survivors. But, causal flow was significantly stronger after MP+PT. Furthermore, causal flow after MP+PT was also found to be significantly stronger than after MP only. We also found that the FMA scores were significantly higher following intervention (MP+PT) in post-stroke hemiplegic patients indicating a greater degree of recovered upper limb function in this group. There was a

correlation, which tended towards significant value, between difference in FMA scores and difference in directed functional connectivity measures from SMA to LPMC following stroke and when the stroke-survivors underwent MP+PT.

4.4.1 Low-frequency network activity

Intrinsic functional networks usually show coherent oscillatory activity in the low frequency band, less than 0.1 Hz. Spontaneous synaptic activity of neurons is known to give rise to fluctuations in fMRI BOLD signals. These low-frequency oscillations are believed to mediate long-distance synchronization of distributed brain regions, modulation of which represents cortical excitability [3,4,69]. Further evidence points to the notion that these oscillations have a definite neuronal basis rather than the result of physiological artifact [4,88,89]. The resting-state activity and the spontaneous fluctuations also reflect the dynamic self-organizing nature of brain [90]. The power of such low-frequency fluctuations of brain signals may differ significantly between stroke survivors and able-bodied healthy individuals [91], which is consistent with our results. Tsai and colleagues [92] reported that during the resting-state, the amplitude of low frequency oscillations is altered in people with impaired consciousness following a stroke. Significant differences in the amplitude of low frequency oscillations was also reported during resting-state in the brain areas of people suffering from depression [93].

However, it has been postulated that following a stroke, brain network activity may deviate. Fluctuations with frequency less than 0.1 Hz have been shown to contribute to resting-state functional connectivity in auditory, visual and motor cortices [88]. Strong coherence relationship between motor areas have been found in the frequency band 0.02-0.15 Hz during rest as well as in the presence of lesions [94]. Dominance of ultra-low frequency band (0.01-0.06 Hz) in cortical

networks and of 0.01-0.14 Hz in limbic networks suggest the involvement of distinct frequency bands in the resting-state fMRI signals [95].

4.4.2 Altered functional connectivity following stroke

Detailed descriptions of resting-state connectivity in stroke survivors may help rehabilitation scientists recognize and target insulted neural networks with evidence-based therapies. It has been suggested that coupling between distinctive cortical areas and their functionality following stroke can be better understood in the absence of any active task [7]. The degree of network disturbance and reduction in network activity following stroke is mainly caused by weak or abnormal neural coupling between higher order pre-motor and motor areas and is dependent on the age, location of lesion and intensity of anatomical damage. Stroke may also leave a strong negative impact on the coupling between the cortex and spinal cord and among cortical areas, which are contiguous or removed from the location of lesion. Our findings are consistent with a dynamic causal modeling (DCM) study by Rehme and colleagues, where changes in effective connectivity within M1, PMC and SMA were observed following stroke [96] in which a reduction in positive coupling of SMA and PMC with M1 was reported. In another DCM study of 12 sub-acute stroke patients during a hand movement task, Grefkes and colleagues found intra-hemispheric and interhemispheric disturbances due to subcortical lesions [97]. They reported that the intrinsic neural coupling between SMA and M1 was significantly reduced in patients recovering from stroke. The deficiency in motor skills due to a single subcortical lesion was thought to be related to pathological interhemispheric interactions among core motor regions. In comparison to able-bodied participants, weaker paths weights have been found from PMC to M1 for stroke patients [98]. Patients with stroke had significantly diminished connections between fronto-parietal cortices and primary motor areas, suggesting an overall weaker

confirmatory model. Our findings also showed a significantly diminished motor network compared to healthy participants. In addition, abnormal effective connectivity has been shown between PMC, SMA and prefrontal cortex in patients with Parkinson's disease due to disturbed functionality of a subcortical circuit [99].

4.4.3 Recovered functional connectivity following rehabilitation

Several studies on animals and humans provide insight demonstrating the basis of recovery mechanisms. Studies in rodent models have shown multiple cellular level changes occur in the unaffected hemisphere during recovery from stroke [100]. A study on non-human primates have shown that the degree of motor impairment after stroke depends upon the damage to direct corticospinal connections between neurons in motor areas M1, PMC and SMA and alpha-motor neurons [101]. Motor recovery may be associated with increased activation in the SMA [102]. Various hypotheses have been proposed describing the source of activations in SMA. It is believed that without execution of a motor plan, MP or mental rehearsal forms a hypothetical environment of movements, which causes activation of motor preparation or motor execution network [61]. Lotze and colleagues (Lotze, et al. [103]) in an fMRI study of healthy participants have verified this observation, where supplementary motor area (SMA), premotor cortex (PMC) and primary motor area (M1) are found to be consistently active during motor execution as well as during motor imagery task. Activation of the same neural populations during MP and physical actions may be because of the same vegetative responses elicited by both [13]. Performance times are also found to be close for imagined and physically performed tasks with different levels of difficulty [104,105]. Treatment by MP, which is fundamentally rehearsal of an action mentally without any physical effort, is usually considered as mental imagery (MI) task. Only slight but insignificant restoration of insulted brain

networks following MP has been observed in the current study which may be because both motor-imagery and motor-execution are known to associate with similar brain networks. Brain studies have confirmed a correspondence between imagined and executed movements and considered MI as a dynamic process with a strong correlation with motor-execution. Mental rehearsal by itself or in combination with physical practice has been proven to be beneficial for healthy as well as for mentally challenged individuals [15,106]. Our report that MP with motor imagery may cause the internal simulation of movements but not enough to match with young able-bodied participants whereas repetitive physical practice combined with MP causes a stronger cortical reorganization and improved functional interactions is consistent with previous findings [13,107]. Our findings of the directed functional connectivity changes for stroke patients following rehabilitation are consistent with a study by Rehme and colleagues who also reported an increase in coupling between SMA, M1 and PMC following rehabilitation [96]. SMA and PMC are found to have direct extensive projections to M1 in non-human primates [108] and may play a critical role in motor recovery. Findings from a study by James and colleagues suggested that the unaffected hemisphere has a strong and direct influence on the affected hemisphere following stroke, but this influence diminishes with recovery [5]. Despite the variability due to heterogeneity of lesion locations in our sample of aged stroke-survivors, our current findings suggest a significant influence of rehabilitation therapy such as MP+PT on motor networks and upper limb motor recovery in post-stroke hemiplegic patients.

Previous studies [13,109,110] have shown that the combination of MP and PT is helpful in improving functional and motor skills more than PT only. MP by itself is considered an effective technique to enhance motor performance by tracing the overlap between motor imagery and motor execution neural circuits [111]. Although, the improvement in muscular strength of participants with

deficiency in motor skills following MP is less than physically trained participants [112]. We found that the combination of MP and PT significantly improved the connectivity between specific cortical areas as well as for motor-execution network as a whole and tended towards connectivity values of healthy participants. These findings are in-line with our behavioral results where we reported that the FMA scores for patients who received MP+PT are significantly higher than before intervention. Differences in FMA scores and GC values before and after MP+PT also follow a linear trend. Page and colleagues also observed that the patients who received MP+PT improved significantly by an average of 7.81 and 6.72 points on the Action Research Arm (ARA) test and Upper Extremity Fugl-Meyer Assessment of Motor Recovery After Stroke (FM) respectively whereas patients who received PT and relaxation showed significantly lower scores of only 0.44 points and 1 point on the ARA and FM respectively [113].

We also found that there was decrease in causal flow values from SMA to RM1, RPMC to LM1 and RPMC to SMA after MP. The decrease in causal values was less when aged stroke patients underwent MP+PT. The decrease in value could be because mental practice or imagery usually consists of a set of relatively independent processing sub-systems [114,115]. Lack of simultaneous activations in these sub-systems may result in weakening of the connections in motor network. Mental practice may also involve some manipulation, producing descriptions of the task or daydreaming [114,116]. Hence, whether and how long these weak interactions arising from mental practice are retained is an interesting question for future investigations.

Limitations: Lesion locations in our sample of participants were not homogeneous. This may have added variability to the connectivity measures for some of the regions of interest.

The sample included stroke survivors with a wide age and time since stroke, hence further adding to intersubject variability. Future studies having participants with age-matched stroke and able-

bodied volunteers can provide better references for brain connectivity comparisons and may give better estimates of connectivity improvements comparable with able-bodied patients. Despite the variability and this limitation, our data show excellent correlation between brain network activity flow and behavioral measures within the recovering stroke patients of similar age group.

4.4.4 Conclusions

In conclusion, the results of the current study suggest that the fMRI BOLD brain signals can capture the network activity flow changes within the cortical motor-execution network following stroke and during the course of rehabilitation and recovery. The combination of mental practice and physical therapy is an effective treatment option, capable of producing significant behavioral and brain activity changes. The directed functional connectivity approach allows us to probe the brain network mechanisms during the course of motor recovery from stroke, providing the basis for clinical decisions making and selection of treatments for stroke patients.

5 EFFECTIVE CONNECTIVITY DURING MOTOR-IMAGERY AND MOTOR-EXECUTION FOLLOWING STROKE AND REHABILITATION

5.1 Introduction

Motor-imagery and motor-execution tasks have been used to study motor recovery in people following stroke [13,15,117,118]. Previous studies have investigated the effects of stroke on motor networks [5,14,110,119] but there is little data on the effects of interventions on motor behavior and motor network interactions. Here, by using a dynamical causal modeling (DCM) approach [21,44,120], we investigated effective connectivity among three motor areas: the primary motor cortex (M1), the pre-motor cortex (PMC) and the supplementary motor area (SMA), which are known to interact

during motor-execution and imagery tasks. As described in previous chapters, mental practice (MP) and physical therapy (PT) are used frequently to improve motor function for people recovering from stroke. The primary goal of such treatments is to help patients regain motor strength or function that was completely or partially lost due to stroke. Once again, in the current study, we used either MP or combination of MP and PT. MP is defined as use of internal simulation that originates by creating an experience but without any overt movements [13,106]. PT involves actual physical exercise, which has been demonstrated to improve learning and restoration of lost skills in stroke survivors.

Several studies have reported that cortical activation during MP are identical to PT [121,122]. In a study by Althschuler and colleagues [123], a comparison was done between movements of the impaired and the healthy arm; they found that several patients regained function of their affected arm when they watched the reflection of their healthy arm moving in a mirror, which may be regarded as a MP task. Recently, a combination of MP and PT has emerged as an effective tool to improve and characterize brain functionality at various stages following stroke [1,13]. It has been mentioned that following intervention PMC develops functional interactions with ipsilesional M1 [124,125]. Although the source of the neuronal change associated with these interventions remains unclear. There is debate as to whether an intervention promotes the promulgation of same neuronal population during recovery period or intervention recruits other neuronal populations to compensate for the role played by affected neurons. A few studies [126,127] have shown that repetitive task performance may lead to an increase in motor-map size in the affected hemisphere and this might be associated with a shift in laterality of motor cortical activation from damaged to undamaged hemisphere.

Brain activation and effective connectivity have been extensively studied in healthy people using motor-imagery and motor-execution tasks. Motor-imagery tasks (mental rehearsal) can involve a representation of movements in the brain [57,128]. The extent and distribution of activations may differ in motor-imagery and motor-execution, but both motor imagery and motor execution tasks activate the network that involves the core motor areas: M1, SMA and PMC [3,56,58,59,62]. These areas are known to be involved in planning, initiation and execution of motor commands. The roles of SMA and PMC have been reported repeatedly during motor-imagery as well as during motor-execution tasks. They send neuronal impulses to M1. Several studies on effective connectivity and directed functional connectivity have reported the interactions of these areas within themselves as well as with areas such as: basal ganglia, putamen, cerebellum, inferior and superior parietal lobule and other somatosensory areas [58,129-131] whereas SMA, M1 and PMC are also known to be anatomically connected [47,129].

In the present study, our analysis of brain effective connectivity within motor network of stroke patients is based on dynamical network modeling (DCM) [21]. We hypothesized that either MP or MP + PT would strengthen the effective connectivity on the affected side of the brain's motor network as patients regain motor ability. We tested this hypothesis by formulating several models using DCM using ordinary differential equations and compared the exceedance probability of each model. Exceedance probability represents the degree of belief about a model having higher posterior probability than the remaining models [51]. We also explored and compared the role of M1 in affected and unaffected hemispheres during motor-imagery and motor-execution tasks.

5.2 Materials and methods

5.2.1 Participants and pre-scan measures

We recorded fMRI data from 13 adult stroke survivors. Data from three subjects following intervention were not recorded properly and were excluded from the analysis. Four (2 females, 2 males) of the remaining 10 participants (4 females, 6 males) had left hemiparesis resulting from infarct or hemorrhage located in the thalamus, basal ganglia, caudate and pontomedullary. The remaining six volunteers had right hemiparesis due to infarctions of the middle cerebral, pontine or internal carotid arteries (Table 4.1) [8]. The mean age of the participants was 60.10±10.52 years. All the participants were independent in standing, toilet transfer, could maintain balance for at least 2 min. with arm support and met the criterion of being at-least 18 years old. Upper extremity movement criteria included the ability to actively extend the affected wrist ≥20° and extend 2 fingers and thumb at least 10° with a motor activity log (MAL) score of less than 2.5 [82]. Either MR imaging or computed tomography (CT) was used to confirm the stroke location (Table 4.1). Stroke latency ranged from 1 to 54 months. The Mini-Mental State Exam (MMSE) [83], Fugl-Meyer Motor Assessments (FMA) [84] and MIQ-RS (movement imagery questionnaire-revised for stroke) [132] were used to assess cognitive aspects of mental function, sensation and motor function, and motor-imagery (kinesthetic and visual) ability respectively (Table 4.1). The MMSE consisted of two sets of questions; the first tested orientation, memory and attention whereas the second set tested the participant's ability to name, follow verbal and written commands, write a sentence spontaneously and copy a complex polygon. A maximum score of 30 is indicative of normal cognitive function. The FMA included a total of 33 items including: reflexes, volitional movement assessment, flexor synergy, extension synergy, movement combining synergies, movement out of synergy, normal

reflex assessment, wrist movement, hand movement, co-ordination and speed, each with a scale from 0-2 (0 for no performance, 1 for partial performance and 2 for complete performance). The total possible score was 66 where a score of nearly 33 represents moderate impairment of the affected upper limb. The MIQ-RS assesses how well people are able to mentally perform movements and consisted of everyday movements e.g. bending, pushing, pulling and reaching for and grasping [132,133]. Participants rated the level of ease/difficulty on a 7-point scale from 1 = very hard to see/feel to 7 = very easy to see/feel [110].

5.2.2 Tasks

All participants were instructed to lay supine in the scanner with both arms outstretched close to their body. A block-design paradigm was used to run the task, which consisted of four runs [110]. Each run consisted of three stimulation blocks with an alternate 30 seconds period of passive rest. During the motor-imagery task, participants were instructed: 1) To track a sinusoidal wave while imagining the movement of the fingers of unaffected hand, called 'imagine unaffected (IU)' task and 2) To repeat the same task but now imagining the movement of fingers of affected hand, called 'imagine affected (IA)' task. During the motor-execution task, participants were instructed: 1) To track the same sinusoidal wave by continuously pinching a force transducer between thumb and index finger of the unaffected hand, called 'pinch unaffected (PU)' task and 2) To repeat the task with affected hand, called 'pinch affected (PA)' task. By providing visual feedback to the participants, we made sure that the participants performed the task as accurately as possible. Stroke patients practiced the tasks outside the scanner as well. As reported previously by Confalonieri and colleagues [110], the relative root mean squared error (RRMSE) was very close to zero, which suggested a good control of grip force modulation. Also, time spent within target range (TWR)

close to 30 s suggested a normal level of accuracy on matching the target force and the coefficient of co-ordination (K_c) close to 1 reflected normal coordination of grip force.

Four stroke-survivors had an affected left hemisphere and six had an affected right hemisphere. We separated data for left and right hemisphere, resulting in total 8 sets of data for each participant:

(a) **Motor-imagery - imagine unaffected (IU):** (1) Four participants have right hemisphere unaffected and (2) six have left hemisphere unaffected.

(b) **Motor-imagery - imagine affected (IA):** (3) Six participants have right hemisphere affected and (4) four have left hemisphere affected.

(c) **Motor-execution - pinch unaffected (PU):** (5) Four participants have right hemisphere unaffected and (6) six have left hemisphere unaffected.

(d) **Motor-execution - pinch affected (PA):** (7) Six participants have right hemisphere affected and (8) four have left hemisphere affected.

5.2.3 Imaging

MR imaging was done using a Siemens 3.0 T Magnetom Trio scanner (Siemens Medical Solutions, Malvern, PA, USA) with a standard quadrature head coil and with TR/TE/FA=2350 ms/28 ms/90°, 130 time points (~5 min each), resolution=3x3x3 mm^3 and 35 axial slices. An anatomical image of each participant was acquired using a 3D magnetization-prepared rapid acquisition gradient echo (MPRAGE) sequence which consisted of 176 sagittal slices of 1 mm-thickness (resolution = 1x1 mm, in-plane matrix = 256x256) with TR/TE/FA/inversion time of 2300 ms/3.02 ms/8°/1100 ms. All stroke survivors underwent two tasks based scanning sessions. The delay between the scanning sessions ranged from 14-51 days. The second session was

executed following an intervention where all the stroke survivors underwent either mental practice (MP) therapy or combined mental practice and physical therapy (MP+PT).

5.2.4 Intervention details

See section 4.2.3.

5.2.5 FMRI preprocessing

FMRI data were preprocessed by using SPM8 (Wellcome Trust Centre for Neuroimaging, London; http://www.fil.ion.ucl.ac.uk/spm/software/spm8/). The preprocessing steps involved slice time correction, realignment, normalization and smoothing. Motion correction to the first functional scan was performed within participant using a six-parameter rigid-body transformation. Six motion parameters (three translational and three rotational) were stored and used as nuisance covariates. The mean of the motion-corrected images was then coregistered to the individual structural image using a 12-parameter affine transformation. The images were then spatially normalized to the Montreal Neurological Institute (MNI) template [134] by applying a 12-parameter affine transformation, followed by a nonlinear warping using basis functions [86]. Images were subsequently smoothed with an 8-mm isotropic Gaussian kernel and the low-frequency drifts in signal were removed using a standard band-pass-filter with a 128 seconds cutoff.

5.2.6 Volumes of interest (VOIs)

We defined volumes of interest for three basic motor areas- the primary motor cortex (M1), the premotor cortex (PMC) and the supplementary motor area (SMA) in SPM8 using the first eigen-variate of activations within a sphere of 8 mm radius centered at (-33, -19, 52), (36, -18, 52), (-34, -1, 56), (35, 0, 55) and (0, -4, 65) in MNI coordinate system for the left M1, the right M1, the left PMC, the right PMC and the bilateral SMA respectively. In accordance with literature [135], VOIs

were defined by extracting mean time-series from same set of voxels across the participants for each VOI corresponding to each of the four conditions. For that, we avoided any statistical threshold on activity within areas of interest so that extracted and adjusted time-series data remain spatially identical across all the participants [135]. Along with some disadvantages e.g. condition independent noise, there are several advantages supporting the use of this technique. None of the participants was excluded from the DCM analysis even if activation in the areas of interest did not reach a pre-defined threshold ($p < 0.01$). A requirement for DCM is that all three VOIs were defined subject-wise according to next local maximum for affected and unaffected hemispheres. The participant specific maxima were constrained to lie within twice the width of Gaussian smoothing kernel [136,137].

5.2.7 Dynamical causal modeling (DCM)

In the current DCM study, we proposed a basic motor network model (model 1, Fig. 5.1) consisting of three motor areas: M1, PMC and SMA with bidirectional endogenous connections among them all. This corresponds to endogenous connectivity matrix, A, which is based on previous anatomical references for these three areas [14,47,66,138,139]. This basic model was elaborated into 7 more different models depending upon which endogenous connections from SMA and PMC were modulated by the external experimental input (represented by the term 'TASK' in Fig. 5.1), which can be either of IU, IA, PU and PA. Thus, for each condition, we proposed 8 models for each hemisphere (affected and unaffected), which sum to 64 models (32 before intervention and 32 after intervention) for each participant and each hemisphere. All the models were defined and estimated using a bilinear approach [21]. We attempted to keep the model space as simple as possible and

avoided including any complex model in order to maintain the balance between accuracy and complexity [41,140].

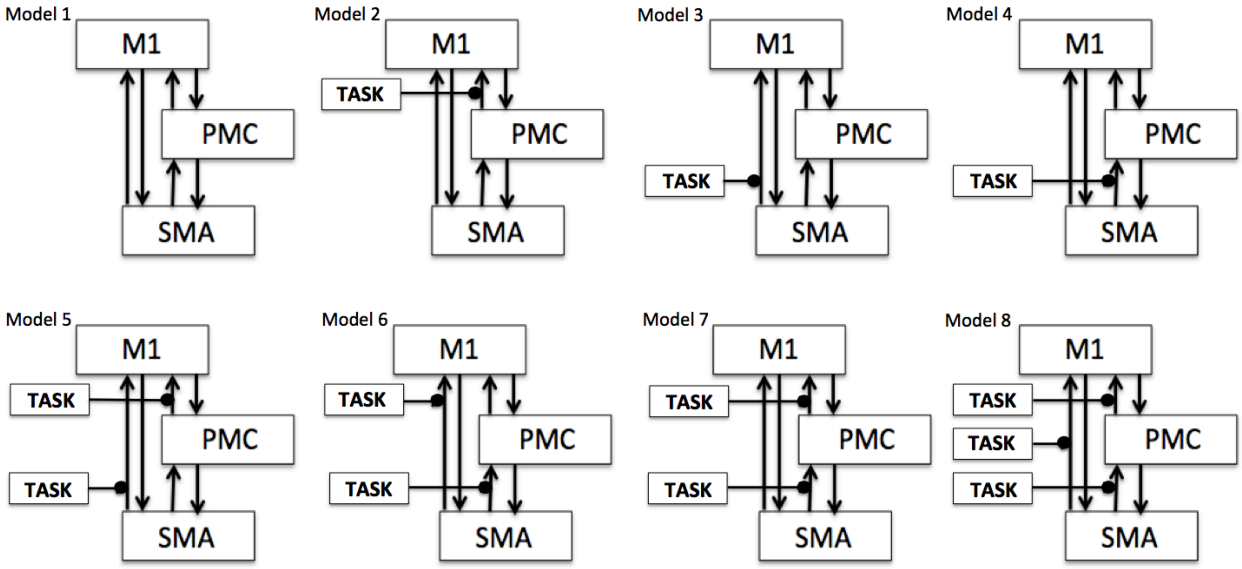

Figure 5.1 Model space specification.

Eight models (model 1 - model 8) are specified constituting bilinear family for each condition. Here 'TASK' represents (1) imagine unaffected (IU) (2) imagine affected (IA) (3) pinch unaffected (PU) and (4) pinch affected (PA) condition for left (unaffected and affected) and right hemisphere (unaffected and affected).

5.3 Results

5.3.1 Effective connectivity

5.3.1.1 Optimal model selection

Considering areas from both unaffected (left and right) and affected (left and right) hemispheres, we calculated exceedance probabilities of all eight pre-defined models (model 1-model 8) (Fig. 5.1) of bilinear family using BMS RFX criterion. Exceedance probabilities of first two optimal models for each condition before and after intervention are shown in Table 5.1(a).

(a) Motor-imagery: before and after intervention

Unaffected hemisphere: For the left hemisphere, we found the same model 1 as the optimal model before and after intervention (Figures 5.2A-B). For the right hemisphere, model 2 was the optimal model before intervention (Fig. 5.2C) and model 6 was the optimal model after intervention (Fig. 5.2D). Hence for IU condition, overall we found model 1 was the optimal model before as well as after the intervention (Table 5.1(a)).

Affected hemisphere: For the left hemisphere, we found model 7 was the optimal model before intervention (Fig. 5.3A) and model 3 was the optimal model after intervention (Fig. 5.3B). For the right hemisphere, model 4 was the optimal model before intervention (Fig. 5.3C) and model 2 was the optimal model after intervention (Fig. 5.3D). Hence for IA condition, overall we found model 7 was the optimal model before intervention and model 3 was the optimal model after intervention (Table 5.1(a)).

Table 5.1 Optimal model selection and modulatory parameters for dominating models.

(a) The best model is selected by comparing model exceedance probabilities of top two models before and after intervention for each task condition. After intervention, we found the same model (model 1) winning in case of imagery (unaffected) and execution (unaffected and affected) conditions whereas model 3 was winning in case of imagery-affected condition. (b) After intervention, comparing exceedance probabilities of model 1 and model 3, we found model 3 dominating over model 1 in case of IA-right and PU-left task conditions whereas model 1 was dominating over model 3 in case of PU-right task condition. The modulatory parameter for connection from SMA to M1 was negative for IA-right and positive for PU-left task condition. Here dominating models and their modulatory parameters (M.P.) are emphasized in bold.

(a) Optimal model selection

Condition	Hemisphere	Before Intervention			After Intervention			
		Optimal models			Optimal models			
		Model	**E. P.**	**Optimal model (E.P.)**	**Model**	**E. P.**	**Optimal model (E.P.)**	**Optimal model (P.E.P.)**
IU	Left	Model 1 Model 4	0.45 0.17	Model 1 (0.45)	Model 1 Model 3	0.44 0.19	**Model 1** **(0.44)**	**Model 1** **(0.55)**
	Right	Model 1 Model 2	0.18 0.42		Model 1 Model 6	0.26 0.32		
IA	Left	Model 4 Model 7	0.18 0.43	Model 7 (0.43)	Model 3 Model 4	0.35 0.18	**Model 3** **(0.35)**	**Model 3** **(0.31)**
	Right	Model 1 Model 4	0.26 0.36		Model 2 Model 7	0.27 0.19		
PU	Left	Model 3 Model 6	0.26 0.28	Model 3 (0.39)	Model 3 Model 5	0.22 0.27	**Model 1** **(0.31)**	**Model 1** **(0.24)**
	Right	Model 2 Model 3	0.11 0.39		Model 1 Model 4	0.31 0.29		**Model 5** **(0.24)**
PA	Left	Model 1 Model 7	0.17 0.28	Model 1 (0.31)	Model 1 Model 2	0.23 0.26	**Model 1** **(0.37)**	**Model 1** **(0.32)**
	Right	Model 1 Model 8	0.31 0.23		Model 1 Model 3	0.37 0.28		

(b) Model 1 vs. model 3 comparison and modulatory parameters (M.P.) (in Hz) from winning model

Condition	Hemisphere	After intervention				
		Model	**E. P.**	**Optimal model**	**M. P. (mean±s.d.) for SMA to M1**	**Optimal model**

				(E.P.)		**(P.E.P.)**
IU	Left	Model 1 Model 3	0.51 0.49	None	N.A.	None
	Right	Model 1 Model 3	0.49 0.51			
IA	Left	Model 1 Model 3	0.51 0.49	None	N.A.	Model 3 (0.57)
	Right	Model 1 Model 3	0.22 0.78	**Model 3** **(0.78)**	**-0.0111±0.0045**	
PU	Left	Model 1 Model 3	0.07 0.93	**Model 3** **(0.93)**	**0.0254±0.0048**	Model 3 (0.57)
	Right	Model 1 Model 3	0.82 0.18	**Model 1** **(0.82)**	N.A.	
PA	Left	Model 1 Model 3	0.50 0.50	None	N.A.	None
	Right	Model 1 Model 3	0.50 0.50			

IU: Imagine Unaffected; IA: Imagine Affected; PU: Pinch Unaffected; PA: Pinch Affected; E. P.: Exceedance Probability; P.E.P.: Protected Exceedance Probability; MP: Modulatory Parameter; s.d.: standard deviation; N. A.: Not Applicable.

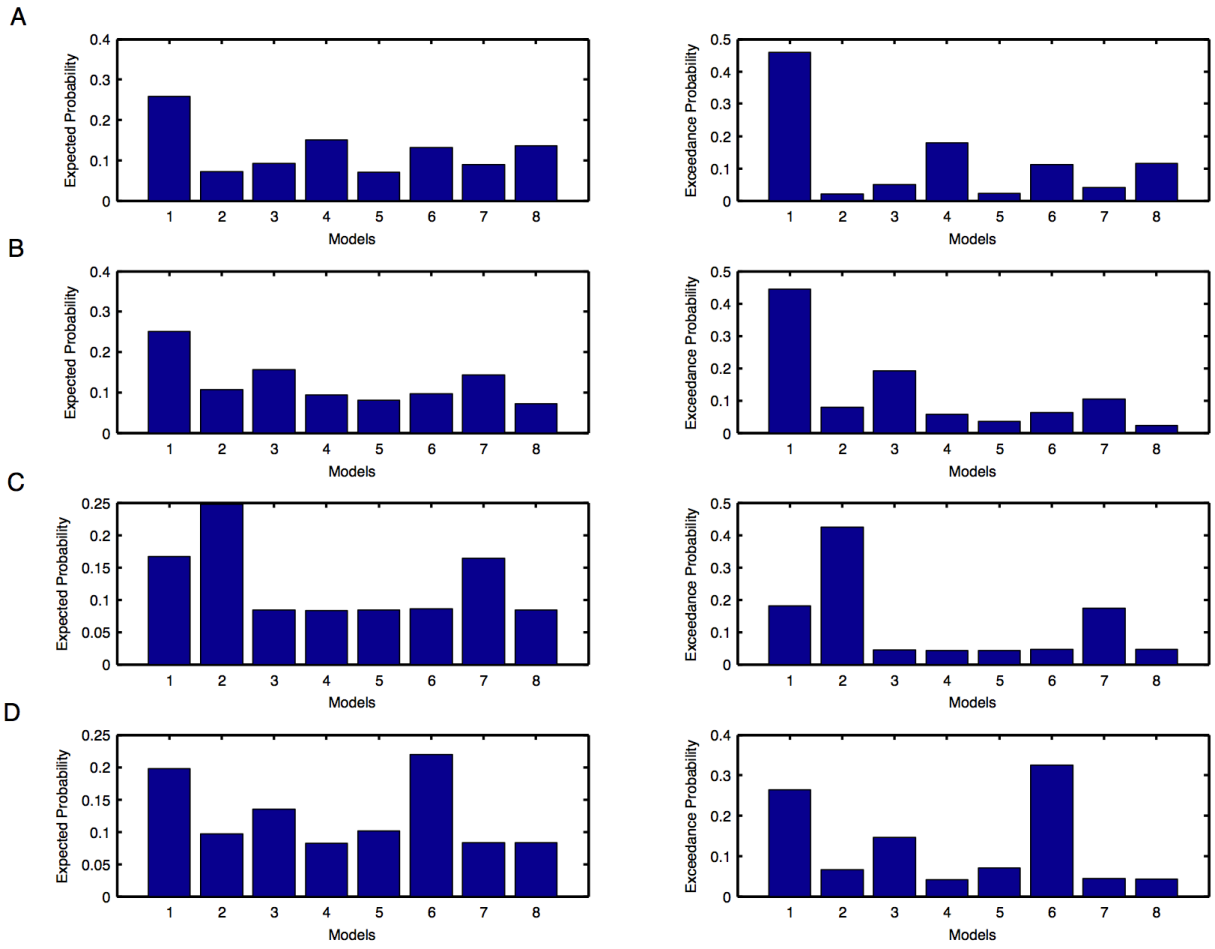

Figure 5.2 Individual model probabilities during motor imagination (MI) task for unaffected hemisphere.

Model expected and exceedance probabilities are shown for each model during MI task for unaffected: (A-B) left and (C-D) right hemisphere. Here probabilities shown in (A, C) are before intervention whereas shown in (B, D) are after intervention.

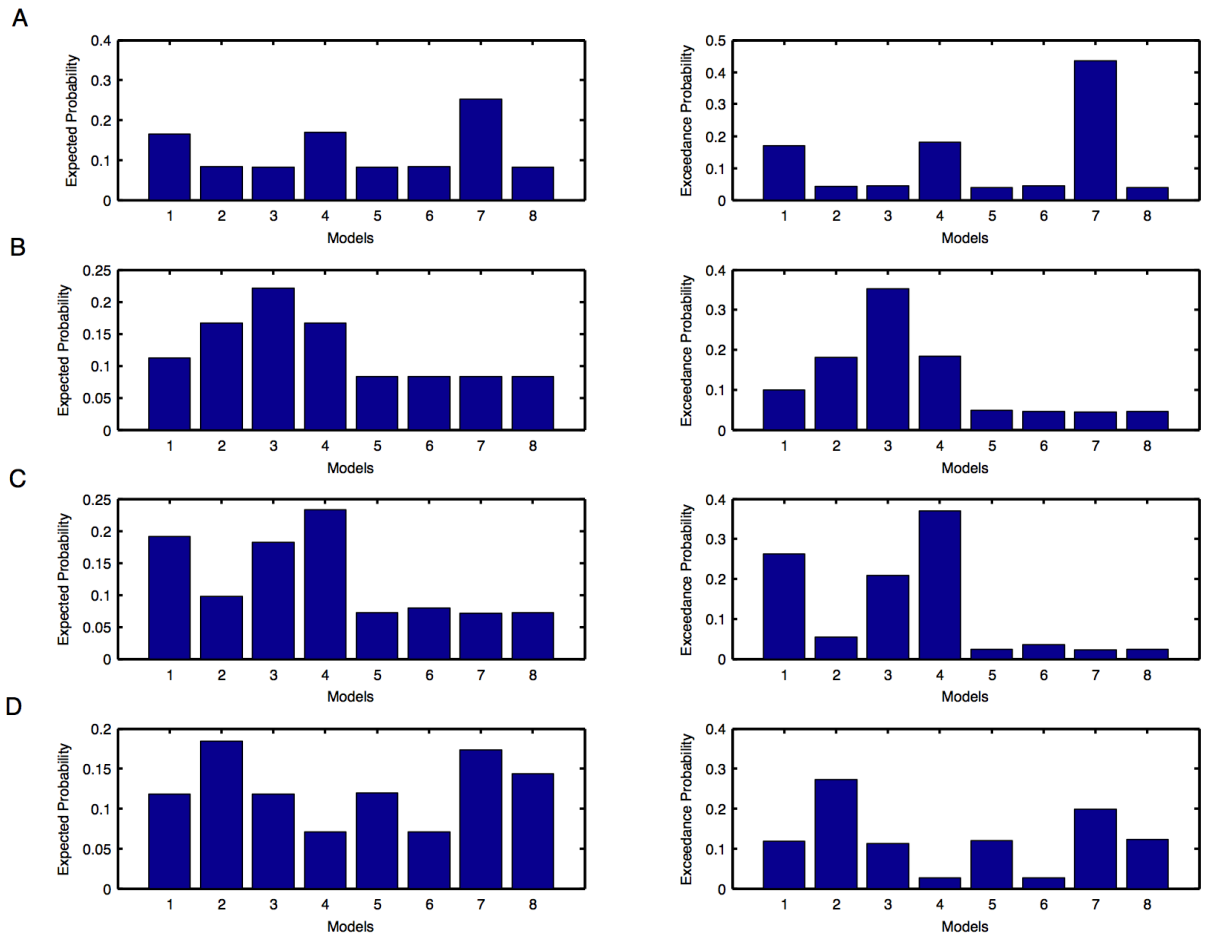

Figure 5.3 Individual model probabilities during motor imagination (MI) task for affected hemisphere.

Model expected and exceedance probabilities are shown for each model during MI task for affected: (A-B) left and (C-D) right hemisphere. Here probabilities shown in (A, C) are before intervention whereas shown in (B, D) are after intervention.

(b) Motor-execution: before and after intervention

Unaffected hemisphere: For the left hemisphere, we found model 6 was the optimal model before intervention (Fig. 5.4A) and model 5 was the optimal model after intervention (Fig. 5.4B). For the right hemisphere, model 3 was the optimal model before intervention (Fig. 5.4C) and model 1 was the optimal model after intervention (Fig. 5.4D). Hence for PU condition, overall we found model 3 was the optimal model before intervention and model 1 was the optimal model after intervention (Table 5.1(a)).

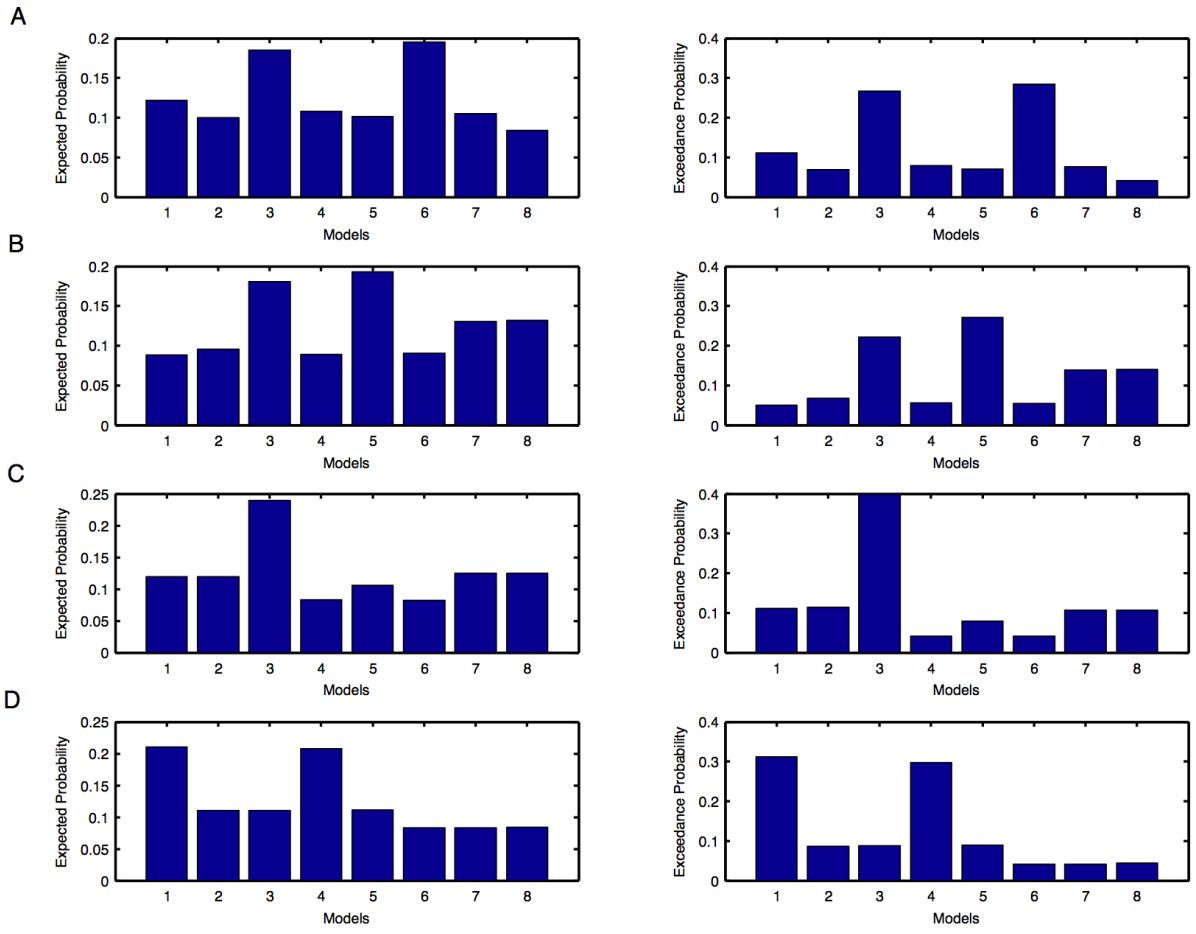

Figure 5.4 Individual model probabilities during motor execution (ME) task for unaffected hemisphere.

Model expected and exceedance probabilities are shown for each model during motor-execution

task for unaffected: (A-B) left and (C-D) right hemisphere. Here probabilities shown in (A, C) are before intervention whereas shown in (B, D) are after intervention.

Affected hemisphere: For the left hemisphere, we found model 7 was the optimal model before intervention (Fig. 5.5A) and model 2 was the optimal model after intervention (Fig. 5.5B). For the right hemisphere, model 1 was the optimal model before as well as after intervention (Figures 5.5C-D). Hence for PA condition, overall we found model 1 was the optimal before and after intervention in the affected hemisphere (Table 5.1(a)).

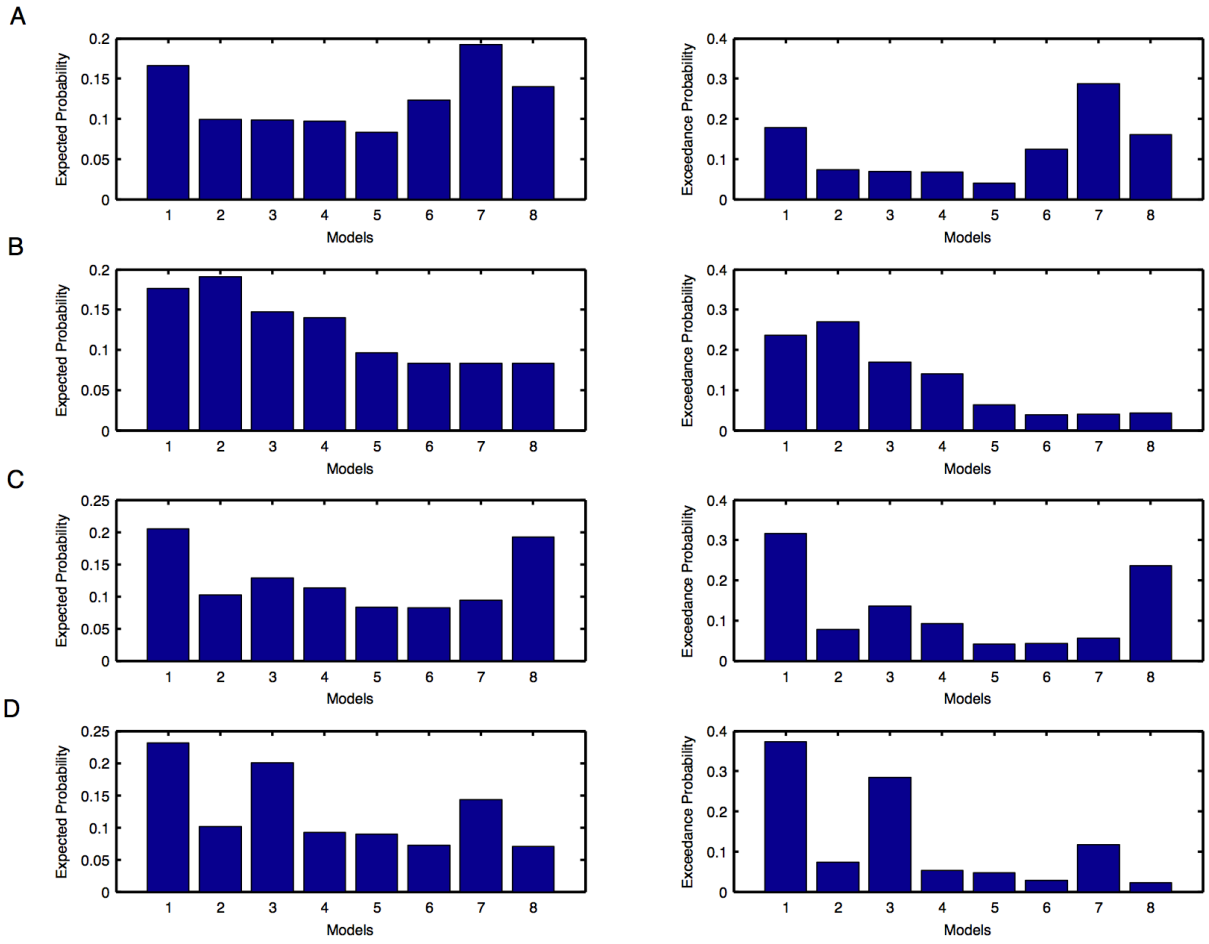

Figure 5.5 Individual model probabilities during motor execution (ME) task for affected

hemisphere.

Model expected and exceedance probabilities are shown for each model during ME task for affected: (A-B) left and (C-D) right hemisphere. Here probabilities shown in (A, C) are before intervention whereas shown in (B, D) are after intervention.

Further, we made sure that the optimal model after intervention for each of the above conditions was consistent with the optimal model found from protected exceedance probabilities calculated by combining left and right hemispheres for corresponding conditions (Table 5.1(a)).

(c) Motor-imagery vs. motor-execution: after intervention

Comparing exceedance probabilities of optimal models (Table 5.1(a)) after intervention for motor-imagery and motor-execution, we found the same optimal model (model 1) for IU, PU and PA conditions and model 3 for IA condition. Since none of the models were clearly winning with an appreciable probability value, we compared model 1 and model 3 for each condition after intervention (Table 5.1(b)). We found that model 3 was the dominant model over model 1 in case of IA-right and PU-left task conditions but model 1 was the dominant model over model 3 for PU-right task condition. Again, we made sure that the optimal model after intervention for each condition was consistent with the optimal model found from protected exceedance probabilities calculated by combining left and right hemispheres for corresponding conditions (Table 5.1(b)).

The modulatory parameter for connection from SMA to M1 was negative for IA-right and positive for PU-left task condition (Fig. 5.6). For other task conditions where we did not find any model clearly winning over the other, we found either highly negative or very weak positive modulation from SMA to M1 during the imagination task but strong positive modulation from SMA to M1 during the execution task.

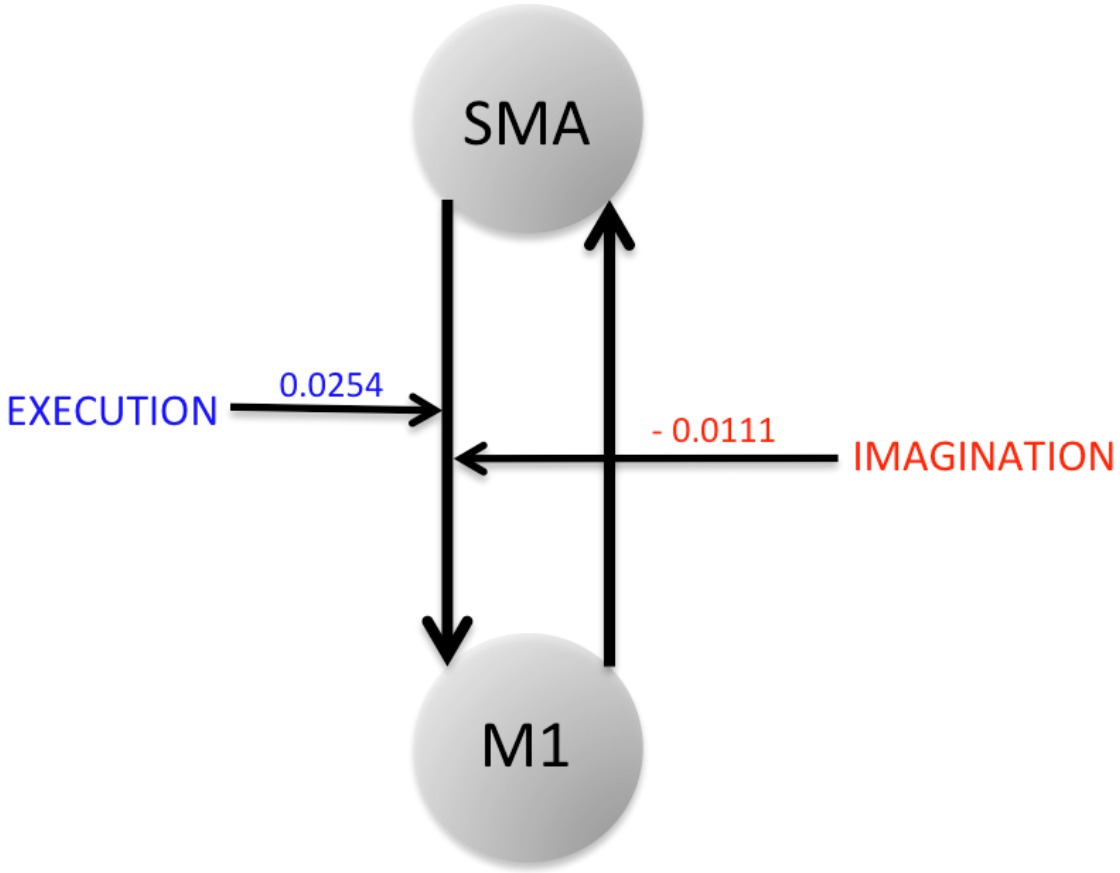

Figure 5.6 Modulatory parameters from optimal model selection.

SMA to M1 connection is positively modulated during motor-execution (ME) whereas the same connection is negatively modulated during motor-imagery (MI). Here optimal model for ME has model exceedance probability of 0.93 whereas optimal model for MI has model exceedance probability of 0.78.

5.3.1.2 Bayesian parameters and significance tests

Using the BMA approach, we calculated the endogenous and modulatory connection strength parameters (in Hz) by averaging over the optimal models of each participant and for each condition,

followed by significance tests. For each connection, the mean of these effective connectivity measures along with standard deviation (SD) and p-value (using one sample t-test) for the left and right hemisphere, before and after intervention for unaffected and affected hemisphere are shown in Table 5.2 for the motor-imagery task and in Table 5.3 for the motor-execution task. Significant connections are marked with an asterisk in Fig. 5.7 and Fig. 5.8. For each condition, we did not consider non-significant connections of both left and right hemispheres.

Table 5.2 Effective connectivity measures.

Endogenous and modulatory connectivity parameters for imagine unaffected (IU) and imagine affected (IA) tasks before and after the intervention.

Connection type	Mean (IU, IA)	SD (IU, IA)	p-value (IU, IA)
Left Hemisphere			
Before intervention			
Endogenous parameters			
PMC→M1	0.144, 0.128	0.021, 0.013	0.051, 0.006*
SMA→M1	0.036, 0.101	0.020, 0.010	0.507, 0.153
M1→PMC	0.158, 0.140	0.021, 0.011	0.037*, 0.008*
SMA→PMC	0.108, 0.190	0.017, 0.010	0.337, 0.033*
M1→SMA	0.074, 0.179	0.022, 0.013	0.315, 0.089
PMC→SMA	0.185, 0.258	0.019, 0.014	0.089, 0.026*
Modulatory parameters			
PMC→M1	-0.005, 0.015	0.018, 0.004	0.721, 0.259
SMA→M1	-0.009, 0.000	0.024, 0.000	0.480, N.A.

SMA→PMC	0.006, 0.038	0.005, 0.004	0.523, 0.145
After intervention			
Endogenous parameters			
PMC→M1	0.166, 0.183	0.013, 0.013	0.012*, 0.009*
SMA→M1	0.109, 0.137	0.011, 0.010	0.016*, 0.026*
M1→PMC	0.190, 0.185	0.014, 0.012	0.030*, 0.004*
SMA→PMC	0.060, 0.165	0.011, 0.010	0.327, 0.036*
M1→SMA	0.174, 0.186	0.014, 0.013	0.023*, 0.066
PMC→SMA	0.084, 0.197	0.014, 0.014	0.278, 0.018*
Modulatory parameters			
PMC→M1	0.021, 0.043	0.006, 0.004	0.227, 0.391
SMA→M1	0.007, -0.006	0.006, 0.005	0.177, 0.334
SMA→PMC	-0.011, 0.002	0.004, 0.001	0.247, 0.391
Right Hemisphere			
Before intervention			
Endogenous parameters			
PMC→M1	0.110, 0.101	0.014, 0.019	0.009*, 0.190
SMA→M1	0.150, 0.099	0.012, 0.018	0.012*, 0.055
M1→PMC	0.122, 0.105	0.010, 0.019	0.030*, 0.156
SMA→PMC	0.234, 0.189	0.011, 0.017	0.004*, 0.003*
M1→SMA	0.180, 0.113	0.011, 0.018	0.024*, 0.080
PMC→SMA	0.270, 0.248	0.013, 0.017	0.001*, 0.000*
Modulatory parameters			

PMC→M1	0.009, -0.000	0.005, 0.001	0.564, 0.363
SMA→M1	0.000, -0.004	0.000, 0.004	N.A., 0.518
SMA→PMC	0.016, 0.011	0.002, 0.005	0.391, 0.053
After intervention			
Endogenous parameters			
PMC→M1	0.148, 0.115	0.010, 0.016	0.042*, 0.019*
SMA→M1	0.128, 0.080	0.009, 0.015	0.014*, 0.178
M1→PMC	0.152,0.115	0.010, 0.011	0.017*, 0.020*
SMA→PMC	0.177, 0.173	0.010, 0.012	0.031*, 0.017*
M1→SMA	0.178, 0.067	0.010, 0.011	0.002*, 0.453
PMC→SMA	0.226, 0.183	0.010, 0.013	0.003*, 0.032*
Modulatory parameters			
PMC→M1	-0.000, 0.039	0.010, 0.064	0.391, 0.319
SMA→M1	0.003, 0.017	0.013, 0.065	0.827, 0.355
SMA→PMC	0.030, 0.003	0.011, 0.005	0.184, 0.795

S.D.: Standard Deviation; N.A.: Not Applicable; $^{*}p < 0.05$.

Table 5.3 Effective connectivity measures.

Endogenous and modulatory connectivity parameters for pinch unaffected (PU) and pinch affected (PA) tasks before and after the intervention.

Connection type	Mean (PU, PA)	SD (PU, PA)	p-value (PU, PA)
Left Hemisphere			
Before intervention			
Endogenous parameters			
PMC→M1	0.215, 0.173	0.012, 0.027	0.000*, 0.028*
SMA→M1	0.002, 0.105	0.011, 0.027	0.978, 0.198
M1→PMC	0.238, 0.142	0.013, 0.028	0.001*, 0.013*
SMA→PMC	0.117, 0.222	0.011, 0.027	0.222, 0.010*
M1→SMA	0.005, 0.143	0.011, 0.026	0.948, 0.037*
PMC→SMA	0.180, 0.239	0.011, 0.028	0.091, 0.002*
Modulatory parameters			
PMC→M1	0.004, 0.005	0.027, 0.121	0.336, 0.345
SMA→M1	-0.008, -0.002	0.021, 0.121	0.313, 0.078
SMA→PMC	0.000, 0.010	0.006, 0.020	0.948, 0.357
After intervention			
Endogenous parameters			
PMC→M1	0.216, 0.192	0.013, 0.027	0.001*, 0.009*
SMA→M1	0.037, 0.173	0.012, 0.026	0.037*, 0.015*
M1→PMC	0.265, 0.217	0.012, 0.027	0.265, 0.018*
SMA→PMC	0.132, 0.111	0.010, 0.026	0.132, 0.227
M1→SMA	0.075, 0.235	0.012, 0.026	0.075, 0.003*
PMC→SMA	0.184, 0.108	0.013, 0.025	0.184, 0.354

Modulatory parameters			
PMC→M1	0.013, 0.005	0.017, 0.039	0.059, 0.170
SMA→M1	0.013, 0.003	0.020, 0.029	0.258, 0.245
SMA→PMC	0.006, 0.000	0.005, 0.004	0.434, 0.423
Right Hemisphere			
Before intervention			
Endogenous parameters			
PMC→M1	0.171, 0.180	0.020, 0.023	0.003*, 0.000*
SMA→M1	0.090, 0.153	0.017, 0.018	0.005*, 0.000*
M1→PMC	0.185, 0.176	0.016, 0.020	0.011*, 0.001*
SMA→PMC	0.236, 0.162	0.015, 0.016	0.002*, 0.001*
M1→SMA	0.116, 0.179	0.020, 0.021	0.006*, 0.000*
PMC→SMA	0.259, 0.196	0.020, 0.022	0.001*, 0.000*
Modulatory parameters			
PMC→M1	0.020, 0.008	0.067, 0.092	0.205, 0.240
SMA→M1	-0.012, 0.012	0.073, 0.077	0.466, 0.127
SMA→PMC	0.004, 0.001	0.005, 0.006	0.391, 0.924
After intervention			
Endogenous parameters			
PMC→M1	0.158, 0.184	0.012, 0.022	0.003*, 0.000*
SMA→M1	0.171, 0.130	0.010, 0.018	0.038*, 0.003*
M1→PMC	0.144, 0.165	0.011, 0.017	0.003*, 0.000*
SMA→PMC	0.161, 0.173	0.010, 0.016	0.110, 0.000*
M1→SMA	0.204, 0.174	0.012, 0.018	0.060, 0.002*
PMC→SMA	0.211, 0.258	0.013, 0.021	0.112, 0.000*

Modulatory parameters			
PMC→M1	0.017, 0.011	0.016, 0.043	0.391, 0.223
SMA→M1	0.006, 0.002	0.012, 0.043	0.391, 0.326
SMA→PMC	-0.006, 0.011	0.003, 0.005	0.449, 0.222

S.D.: Standard Deviation; $^{*}p < 0.05$.

(a) Motor-imagery: before and after intervention

Before intervention: We found that the connection from M1 to PMC was the only significant connection ($p < 0.05$) for IU (Fig. 5.7A) and the connection between SMA and PMC was the only significant connection ($p < 0.05$) for IA (Fig. 5.7B).

After intervention: We found significant bidirectional connections between PMC and M1, and between SMA and M1 ($p < 0.05$) for IU (Fig. 5.7C) and significant bidirectional connection between SMA and PMC, along with connection between PMC and M1 ($p < 0.05$) for IA (Fig. 5.7D).

(b) Motor-execution: before and after intervention

Before intervention: We found that the only significant connection was between M1 and PMC ($p < 0.05$) for PU (Fig. 5.8A) and all the connections except from SMA to M1 were significant ($p < 0.05$) for PA (Fig. 5.8B).

After intervention: We found two significant connections: one from PMC and M1, and other from SMA to M1 ($p < 0.05$) for PU (Fig. 5.8C) and all the connections were significant except between SMA and PMC ($p < 0.05$) for PA (Fig. 5.8D).

(c) Motor-imagery vs. motor-execution: after intervention

In order to find the strongest connection under a particular condition, we eliminated the connections that were not common between the unaffected and affected hemisphere after intervention. We

found that the strongest connection during the motor imagery task was a bidirectional connection between PMC and M1 (Figures 5.7C-D). Similarly, there were two connections, one from PMC to M1 and other from SMA to M1 that were the strongest for the motor-execution task (Figures 5.8C-D). These connections are indicated with blue colored arrows in Figures 5.7 and 5.8.

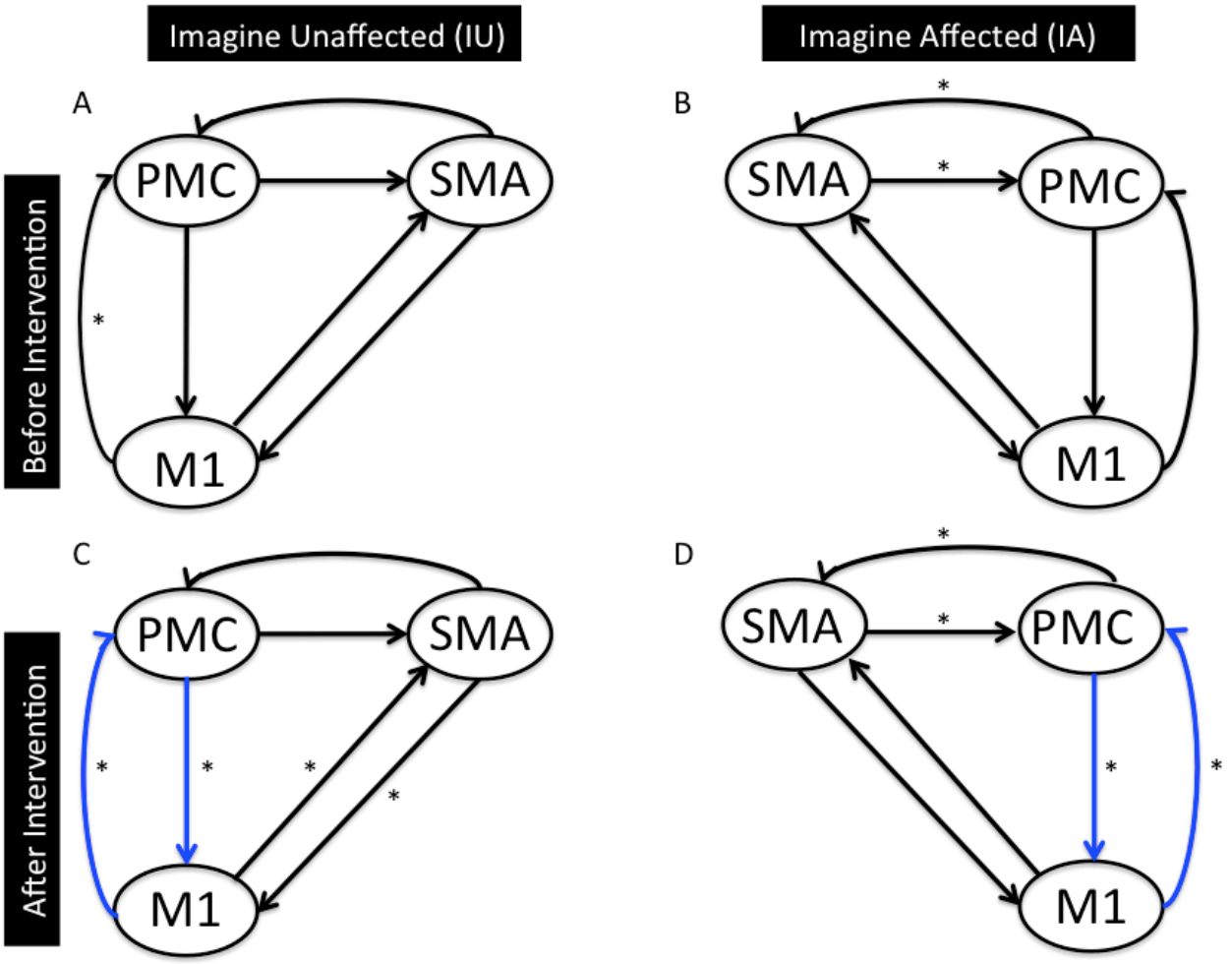

Figure 5.7 Effective connectivity network for motor-imagery (MI) task.

Endogenous connectivity for MI task before (A-B) and after (C-D) intervention is shown. Here significant connections represented by * ($p < 0.05$) are found using one sample t-test. Connections

shown in blue color are common between IU (after intervention) and IA (after intervention).

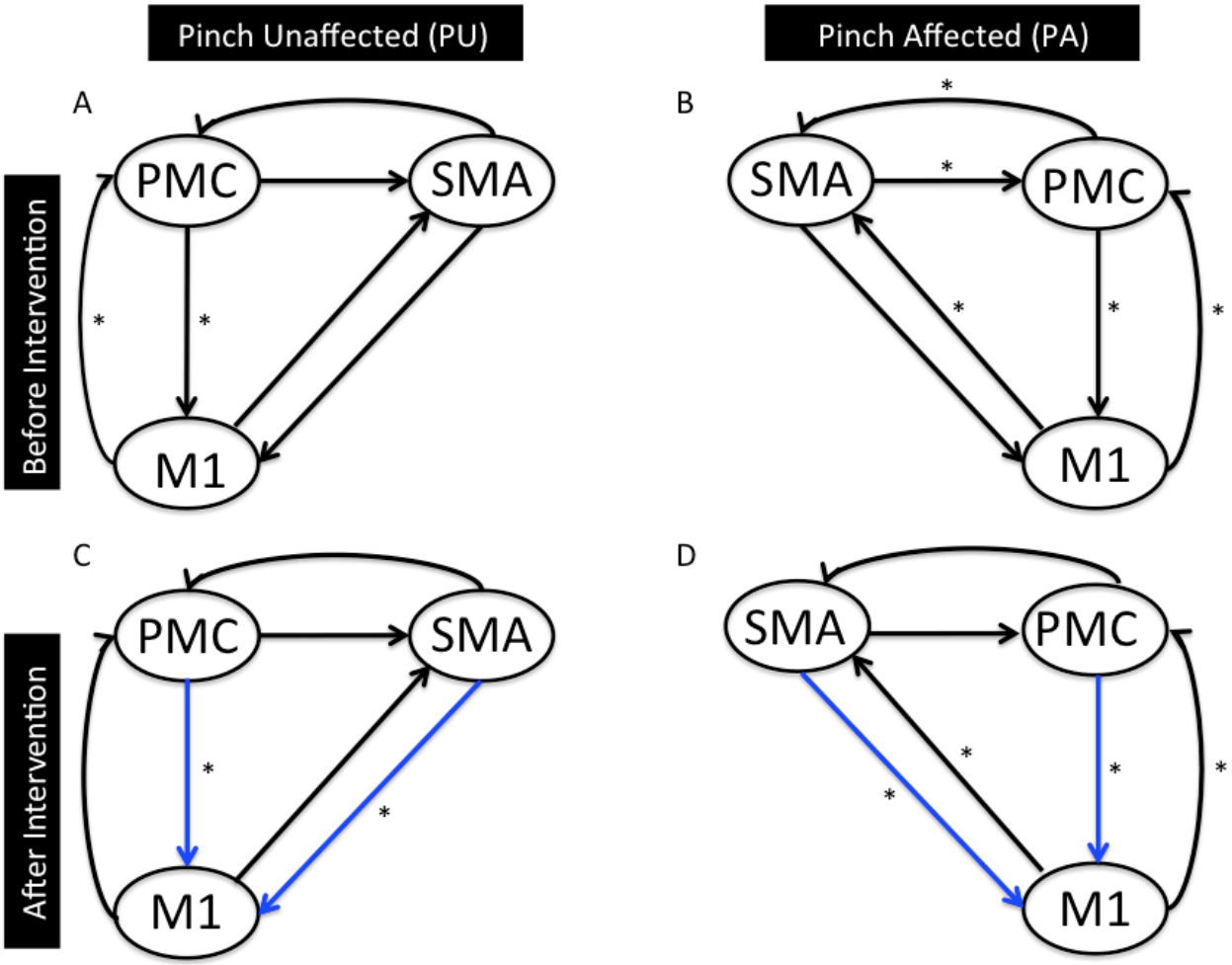

Figure 5.8 Effective connectivity network for motor-execution (ME) task.

Endogenous connectivity for ME task before (A-B) and after (C-D) intervention is shown. Here significant connections represented by * ($p < 0.05$) are found using one sample t-test. Connections shown in blue color are common between PU (after intervention) and PA (after intervention).

5.3.2 Brain and behavior correlation

We recorded FMA scores for all the stroke-survivors before and after intervention. Using paired t-test; we found that FMA scores were significantly higher (sample size = 10; p = 0.001) when the participants underwent a session of intervention (Fig. 5.9).

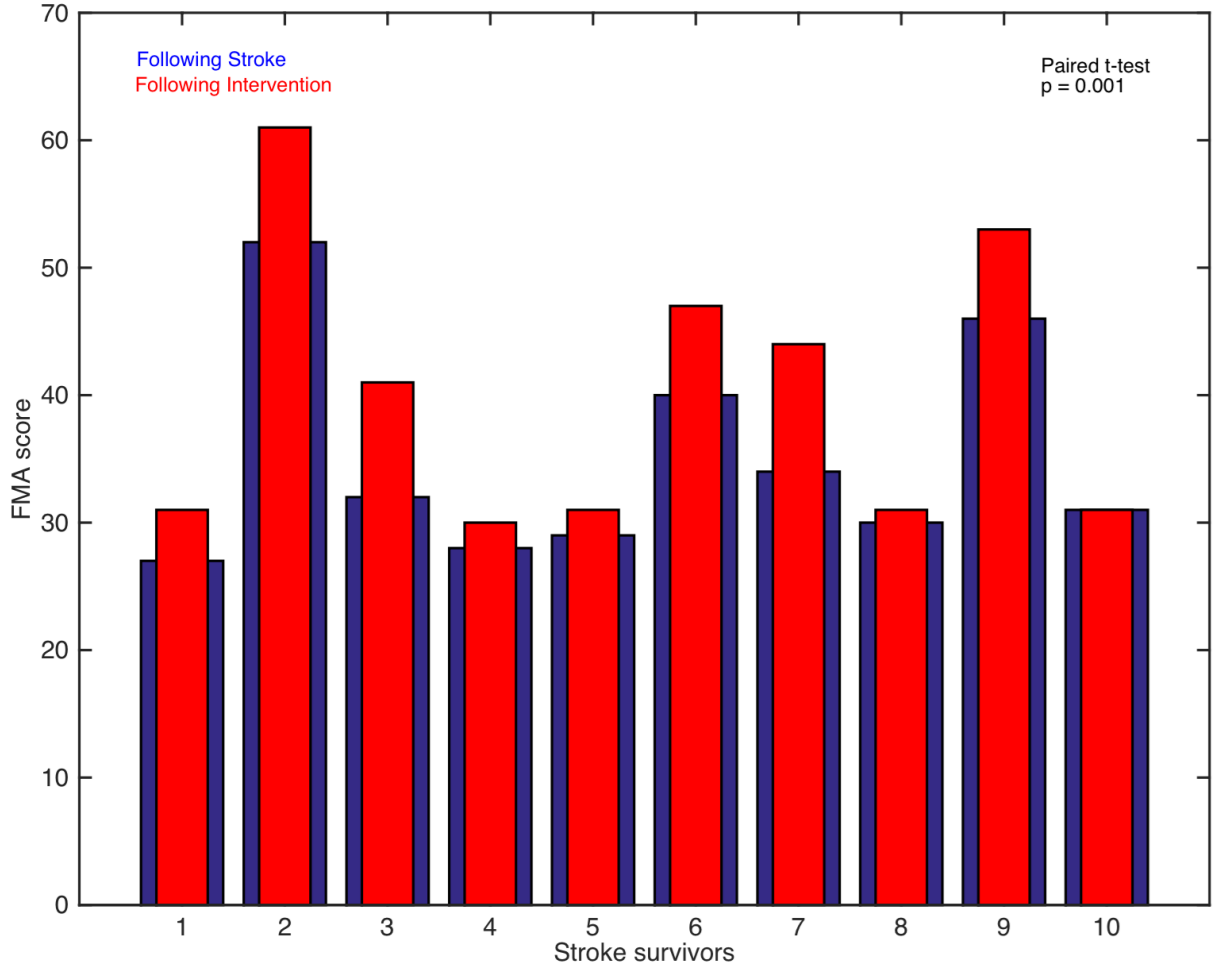

Figure 5.9 FMA scores.

The FMA scores for stroke-survivors following stroke (blue bars) and following intervention (red bars) are plotted.

We also calculated the difference between FMA scores and endogenous connectivity measures before and after intervention. We found a significant linear correlation between the two for the connection from PMC to SMA (correlation coefficient, $r = 0.94$, $p = 0.05$) for the left affected hemisphere during motor-imagery task whereas the correlation for the connection from SMA to PMC under the same condition tended towards significant value (correlation coefficient, $r = 0.88$). Also, the correlation for connection from SMA to PMC for left unaffected hemisphere (correlation coefficient, $r = 0.69$) and from PMC to M1 for left affected hemisphere (correlation coefficient, $r = 0.87$) during the motor-execution task tended towards significance.

5.4 Discussion

In this study, we used a dynamical causal modeling approach on task-based fMRI data to describe the effect of stroke and intervention on the brain. We examined the effective connectivity among numerous cortical areas and found that, after intervention, the optimal models were identical between motor imagery and motor execution tasks for the unaffected hemisphere. Modulatory parameters showed a suppressive (negative) influence of SMA on M1 during the motor-imagery task and an unrestricted (positive) influence of SMA on M1 during the motor-execution task. We also found that for both the hemispheres, intervention caused a reorganization of connectivity patterns among these areas. Inter-regional effective connectivity measures showed that although PMC and M1 were both involved during motor imagery and execution tasks, M1 had a more crucial role along with SMA during the motor-execution task compared to the motor-imagery task. We also report that FMA scores were significantly higher following intervention and there was a significant linear correlation or a correlation which tended towards a significant value between difference in FMA scores and difference in endogenous connectivity measures following stroke and when the stroke-survivors underwent intervention.

5.4.1 Effective connectivity during motor-imagery and motor-execution

Our findings are consistent with several previous neuroimaging studies. Using the BMS approach we found that following an intervention the winning model showed substantial influence of SMA on M1 during motor-imagery as well as during a motor-execution task. Comparing modulatory parameters of both the tasks showed suppressive influence of SMA on M1 during the motor-imagination task and the influence appeared to strengthen the connection from SMA to M1 during the motor-execution task. This suggests that although there were common areas, which were shared between the two tasks, the activated networks differed. Similar findings have been reported that motor-imagination had negative and motor-execution had positive (opposite) effect on the connection from SMA to M1 [47,58,59,131,141-143]. Absence of modulation from PMC to M1 by both tasks reflects weak effective connectivity between PMC and M1. This is consistent with a study by Solodkin and colleagues in 2004 [57]. They reported that a decreased influence of PMC on M1 was accompanied by a stronger influence of SMA on M1 during mental stimulation of movement. The inter-regional effective connectivity measures between SMA and M1 during motor-execution also suggest bidirectional influence between the two which is consistent with a study by Kasess and colleagues [59], who used DCM, to demonstrate a suppressive influence exerted by SMA on M1 with a subsequent feedback influence from M1 to SMA. They reported that SMA may inhibit activity of M1 and may be capable of sustaining activity for several seconds throughout the readiness prior to movement.

Using structural equation modeling, Solodkin and colleagues found motor-imagery and motor-execution tasks activate a basic motor network, yet volumes of activation differ for these two dissimilar tasks [57,144]. Using a conditional Granger causality technique [131], it was shown that more causal information was exchanged during motor-execution than during motor-imagery. This may be

due to some additional neuronal processes occurring because of direct execution of physical movements [145]. By calculating in-out causal flow, these investigators also found that in addition to inferior parietal lobule (IPL) and superior parietal lobule (SPL), dorsal PMC (dPMC) also acted as a causal source in motor-imagery and motor-execution tasks. This is consistent with our findings from the BMA parameters. We find that connectivity between PMC and M1 and from PMC to M1 is stronger during the motor-imagery and motor-execution tasks respectively, whereas there is additional significant connection from SMA to M1 during the motor-execution task. This is consistent with the canonical role of PMC in movement planning which is common between motor-imagery and motor-execution. From inter-regional connectivity measures, we found that PMC is more dominant during the motor-imagery task in comparison to the motor-execution task. This might be because kinesthetic motor-imagery has the capability to boost motor-evoked potentials at the level of premotor areas [14,144,146]. These findings confirmed that although there were overlapping motor areas during motor-imagery and motor-execution, the interaction between SMA and M1 caused more exchange of causal information within motor network during the motor-execution task.

5.4.2 Effect of intervention on effective connectivity

In the present study, BMS results reflect the reorganization of connectivity patterns following intervention. Although the degree of regaining motor skills varies from patient-to-patient depending on the location and extent of lesion [124], stroke patients manage to recover their motor ability. The degree to which motor ability is regained depends on the size of neuronal populations that are thought to reorganize during the intervention period, which may further depend on the intensity of post-stroke therapy. We reported that the intervention significantly improved FMA

scores as well as the connectivity between specific cortical areas. We found that difference in FMA scores and connectivity measures before and after intervention follow a linear trend. These findings are consistent with the findings reported by Page and colleagues [113]. They reported that the mental practice improved scores on the Action Research Arm (ARA) test and Upper Extremity Fugl-Meyer Assessment (FMA) by an average of 7.81 and 6.72 after stroke. Although the mechanism behind recovery of motor skills is not well understood but a well-known notion behind this is that after an effective intervention, the unaffected brain areas undergo structural and functional remodeling and take over the function of affected brain areas by remapping the post functions [124,147,148]. In a study on adult squirrel monkeys by Nudo and colleagues [149], it was reported that monkeys suffering from lesions to motor cortex, could use alternative brain areas to compensate for motor impairments. Arya and colleagues [150] also suggested that motor recovery following rehabilitation could either be: (1) true motor recovery, which comes into play when alternative connections that are undamaged send commands to the same affected muscles to execute the motor commands or (2) compensatory motor recovery which involves sending neuronal commands to alternative but unaffected muscles [151]. In our case, several other factors like task specification e.g. goal-oriented repetitive task practice and a proper environment during rehabilitation might have played significant roles to functionally reorganize the motor networks in order to regain motor ability [150,152]. Task specification may also help engage brain areas that are adjacent to the affected areas [153]. Repetition of task-oriented training has been reported to be more effective [113].

Limitations: Individual behavioral and brain deficit differences following stroke may have added variability to the endogenous and modulatory measures. Despite the variability and small sample size, our data showed a correlation between endogenous connectivity measures and behavioral measures. We did not directly test the functional relevance of unaffected hemisphere for the

changes in regions of the affected hemisphere. However, we found that the connectivity discovered in unaffected hemispheres helps to find the robust connectivity common across affected and unaffected hemispheres after the intervention.

In addition to the findings reported in this study, future effective connectivity studies on a larger pool of stroke patients with a narrow range of stroke intervals and identical stroke locations may provide additional findings.

5.5 Conclusions

In conclusion, the results of the current DCM study describe the disturbances caused in motor network following stroke. Findings reported in this study describe how different motor areas are reorganized after treatment. The roles of PMC and M1 have been specially emphasized during motor-imagery and motor-execution tasks. The inter-regional and network level effective connectivity approaches show the importance of treatments like mental practice and physical therapy during motor recovery and in order to better understand the mechanism behind the recovery process.

6 SUMMARY

Using intrinsic blood oxygenation-level dependent (BOLD) functional magnetic resonance imaging (fMRI) signals from young healthy controls and aged stroke survivors who underwent mental practice only or combined mental practice and physical therapy, we investigated the network activity of five core areas in the motor-execution network consisting of the left primary motor area (LM1), the right primary motor area (RM1), the left premotor cortex (LPMC), the right premotor cortex (RPMC) and the supplementary motor area (SMA).

In the first study, using spectral Granger causality approach, we discovered that during resting state,

(i) the causal information flow between the regions: LM1 and SMA, RPMC and SMA, RPMC and LM1, SMA and RM1, SMA and LPMC, was significantly higher for young healthy controls but was reduced significantly for aged stroke survivors (ii) the flow did not increase significantly after MP alone but (iii) the flow between the regions LM1 and SMA and from SMA to LPMC, after MP+PT increased significantly (iv) sensation and motor scores were significantly higher and correlated with directed functional connectivity measures when the stroke-survivors underwent MP+PT but not MP alone.

In the second study, using dynamical causal modeling approach, we discovered that SMA had a suppressive influence on M1 during the motor-imagery task whereas the influence of SMA on M1 was unrestricted during the motor-execution task. We also found that the connectivity between PMC and M1 was stronger in motor-imagery tasks whereas the connectivity from PMC to M1 and from SMA to M1 dominated in motor-execution tasks. There was also a significant relation between behavioral improvement and a subset of connectivity after intervention.

These studies expand our understanding of motor network involved during three different tasks and two interventions, which are commonly used during rehabilitation following stroke. We conclude that a combination of mental practice and physical therapy can be an effective means of treatment for stroke survivors to recover or regain the strength of motor behaviors. The inter-regional and network level effective connectivity approaches show the importance of treatments like mental practice and physical therapy during motor recovery and in order to better understand the mechanism behind the recovery process.

REFERENCES

1 Bajaj, S., Butler, A. J., Drake, D. & Dhamala, M. Functional organization and restoration of the brain motor-execution network after stroke and rehabilitation. *Front Hum Neurosci* **9**, 1-14, doi:10.3389/fnhum.2015.00173 (2015).

2 Bajaj, S., Butler, A. J., Drake, D. & Dhamala, M. Brain effective connectivity during motor-imagery and execution following stroke and rehabilitation. *Neuroimage Clin* **8**, 572-582 (2015).

3 Bajaj, S., Drake, D., Butler, A. J. & Dhamala, M. Oscillatory motor network activity during rest and movement: an fNIRS study. *Front Syst Neurosci* **8** (2014).

4 Bajaj, S., Adhikari, B. M. & Dhamala, M. Higher Frequency Network Activity Flow Predicts Lower Frequency Node Activity in Intrinsic Low-Frequency BOLD Fluctuations. *PloS One* **8** (2013).

5 James, G. A. *et al.* Changes in resting state effective connectivity in the motor network following rehabilitation of upper extremity poststroke paresis. *Top Stroke Rehabil* **16**, 270-281, doi:10.1310/tsr1604-270 (2009).

6 Wang, L. *et al.* Dynamic functional reorganization of the motor execution network after stroke. *Brain* **133**, 1224-1238, doi:10.1093/brain/awq043 (2010).

7 Grefkes, C. & Fink, G. R. Reorganization of cerebral networks after stroke: new insights from neuroimaging with connectivity approaches. *Brain* **134**, 1264-1276, doi:10.1093/brain/awr033 (2011).

8 Inman, C. S. *et al.* Altered resting-state effective connectivity of fronto-parietal motor control systems on the primary motor network following stroke. *Neuroimage* **59**, 227-237 (2012).

9 Turken, A. *et al.* Cognitive processing speed and the structure of white matter pathways: Convergent evidence from normal variation and lesion studies. *Neuroimage* **42**, 1032-1044 (2008).

10 Granziera, C. *et al.* A new early and automated MRI-based predictor of motor improvement after stroke. *Neurology* **79**, 39-46 (2012).

11 Page, S., Sisto, S. A. & Levine, P. Modified Constraint-Induced Therapy in Chronic Stroke. *Am J Phys Med Rehabil* **81**, 870-875 (2002).

12 Jackson, P. L., Doyon, J., Richards, C. L. & Malouin, F. The efficacy of combined physical and mental practice in the learning of a foot-sequence task after stroke: a case report. *Neurorehab Neural Re* **18**, 106-111 (2004).

13 Butler, A. J. & Page, S. J. Mental practice with motor imagery: evidence for motor recovery and cortical reorganization after stroke. *Arch Phys Med Rehabil* **87**, S2-11, doi:10.1016/j.apmr.2006.08.326 (2006).

14 Sharma, N., Baron, J. C. & Rowe, J. B. Motor Imagery After Stroke: Relating Outcome to Motor Network Connectivity. *Ann Neurol* **66**, 604-616 (2009).

15 Sharma, N., Pomeroy, V. M. & Baron, J. C. Motor imagery: a backdoor to the motor system after stroke? *Stroke* **37**, 1941-1952 (2006).

16 Sharma, N. *et al.* Motor Imagery After Subcortical Stroke: A Functional Magnetic Resonance Imaging Study. *Stroke* **40**, 1315-1324 (2009).

17 Wolf, S. L. *et al.* Effect of constraint-induced movement therapy on upper extremity function 3 to 9 months after stroke: the EXCITE randomized clinical trial. *J Am Med Assoc* **296**, 2095-2004 (2006).

18 Langhorne, P., Bernhardt, J. & Kwakkel, G. Stroke rehabilitation. *Lancet* **377**, 1693-1602 (2011).

19 Friston, K. Functional and Effective Connectivity: A Review. *Brain Conn* **1** (2011).

20 Granger, C., W.,J. Investigating Causal Relations by Econometric Models and Cross-spectral Methods. *Econometrica* **37**, 424-438 (1969).

21 Friston, K. J., Harrison, L. & Penny, W. Dynamic causal modelling. *Neuroimage* **19**, 1273-1302 (2003).

22 Friston, K. J. Causal Modelling and Brain Connectivity in Functional Magnetic Resonance Imaging. *PLOS Biol* **7**, 220-225 (2009).

23 Friston, K. Dynamic causal modeling and Granger causality Comments on: the identification of interacting networks in the brain using fMRI: model selection, causality and deconvolution. *Neuroimage* **58**, 303-305, doi:10.1016/j.neuroimage.2009.09.031 (2011).

24 Zou, C., Katherine, J. D. & Feng, J. Granger causality vs. dynamic Bayesian network inference: a comparative study. *BMC Bioinform* **10**, doi:10.1186/1471-2105-10-122 (2009).

25 Aguirre, G. K., Zarahn, E. & D'esposito, M. The variability of human, BOLD hemodynamic responses. *Neuroimage* **8**, 360-369 (1998).

26 David, O. *et al.* Identifying Neural Drivers with Functional MRI: An Electrophysiological Validation. *PLOS Biol* **6**, 2683-2697 (2008).

27 Schippers, M. B., Renken, R. & Keysers, C. The effect of intra- and inter-subject variability of hemodynamic responses on group level Granger causality analyses. *Neuroimage* **57**, 22-36 (2011).

28 Brovelli, A. *et al.* Beta oscillations in a large-scale sensorimotor cortical network: directional influences revealed by Granger causality. *Proc Natl Acad Sci U S A* **101**, 9849-9854 (2004).

29 Friston, K., Moran, R. & Seth, A. K. Analysing connectivity with Granger causality and dynamic causal modelling. *Curr Opin Neurobiol* **23**, 1-7 (2013).

30 Seth, A. K., Chorley, P. & Barnett, L. C. Granger causality analysis of fMRI BOLD signals is invariant to hemodynamic convolution but not downsampling. *Neuroimage* **65**, 540-555 (2013).

31 Deshpande, G., Sathian, K. & Hu, X. Effect of hemodynamic variability on Granger causality analysis of fMRI. *Neuroimage* **52**, 884-896, doi:10.1016/j.neuroimage.2009.11.060 (2010).

32 Bressler, S. L. & Seth, A. K. Wiener-Granger Causality: A well established methodology. *Neuroimage* **58**, 323-329 (2010).

33 Aquino, K. M., Robinson, P. A., Schira, M. M. & Breakspear, M. Deconvolution of neural dynamics from fMRI data using a spatiotemporal hemodynamic response function. *Neuroimage* **94**, 203-215 (2014).

34 Levin, J. M. *et al.* Influence of baseline hematocrit and hemodilution on BOLD fMRI activation. *Magn Reson Imaging* **19**, 1055-1062 (2001).

35 Levin, J. M. *et al.* Reduction in BOLD fMRI response to primary visual stimulation following alcohol ingestion. *Psychiatry Res* **82**, 135-146 (1998).

36 Noseworthy, M., Alfonsi, J. & Bells, S. Attenuation of brain BOLD response following lipid ingestion. *Hum Brain Mapp* **20**, 116-121 (2003).

37 Feinberg, D. A. *et al.* Multiplexed echo planar imaging for sub-second whole brain FMRI and fast diffusion imaging. *PLoS One* **5** (2010).

38 Wen, X., Rangarajan, G. & Ding, M. Is Granger Causality a Viable Technique for Analyzing fMRI Data? *PLoS One* **8** (2013).

39 Nalatore, H., Ding, M. & Rangarajan, G. Mitigating the effects of measurement noise on Granger causality. *Phys Rev E* **75** (2007).

40 Nalatore, H., Ding, M. & Rangarajan, G. Denoising neural data with state-space smoothing: method and application. *J Neurosci Meth* **179**, 131-141 (2009).

41 Stephan, K. E. *et al.* Ten simple rules for dynamic causal modeling. *Neuroimage* **49**, 3099-3109, doi:10.1016/j.neuroimage.2009.11.015 (2010).

42 Boly, M. *et al.* Connectivity changes underlying spectral EEG changes during propofol-induced loss of consciousness. *J Neurosci* **32**, 7082-7090 (2012).

43 Friston, K., Moran, R. & Seth, A. K. Analysing connectivity with Granger causality and dynamic causal modelling. *Curr Opin Neurobiol* **23**, 172-178, doi:10.1016/j.conb.2012.11.010 (2013).

44 Valdes-Sosa, P. A., Roebroeck, A., Daunizeau, J. & Friston, K. Effective connectivity: influence, causality and biophysical modeling. *Neuroimage* **58**, 339-361, doi:10.1016/j.neuroimage.2011.03.058 (2011).

45 Dhamala, M. in *Encyclopedia of Computational Neuroscience* Vol. 2 (eds D. Jaeger & R. Jung) (Springer, 2014).

46 Dhamala, M., Rangarajan, G. & Ding, M. Estimating Granger Causality from Fourier and Wavelet Transforms of Time Series Data. *Phys Rev Lett* **100**, doi:10.1103/PhysRevLett.100.018701 (2008).

47 Pool, E. M., Rehme, A. K., Fink, G. R., Eickhoff, S. B. & Grefkes, C. Network dynamics engaged in the modulation of motor behavior in healthy subjects. *Neuroimage* **82C**, 68-76, doi:10.1016/j.neuroimage.2013.05.123 (2013).

48 Büchel, C. & Friston, K. J. Modulation of Connectivity in Visual Pathways by Attention : Cortical Interactions Evaluated with Structural Equation Modelling and fMRI. *Cereb Cortex* **7**, 768-778 (1997).

49 Penny, W. D., Stephan, K. E., Mechelli, A. & Friston, K. J. Comparing dynamic causal models. *Neuroimage* **22**, 1157-1172, doi:10.1016/j.neuroimage.2004.03.026 (2004).

50 Stephan, K. E., Penny, W. D., Daunizeau, J., Moran, R. J. & Friston, K. J. Bayesian model selection for group studies. *Neuroimage* **46**, 1004-1017, doi:10.1016/j.neuroimage.2009.03.025 (2009).

51 Wasserman, L. Bayesian Model Selection and Model Averaging. *J Math Psychol* **44**, 92-107, doi:10.1006/jmps.1999.1278 (2000).

52 Rigoux, L., Stephan, K. E., Friston, K. J. & Daunizeau, J. Bayesian model selection for group studies - revisited. *Neuroimage* **84**, 971-985, doi:10.1016/j.neuroimage.2013.08.065 (2014).

53 Penny, W. D. *et al.* Comparing Families of Dynamic Causal Models. *PLOS Comput Biol* **6**, e1000709 (2010).

54 Kasess, C. H. *et al.* Multi-Subject Analyses with Dynamic Causal Modeling. *Neuroimage* **49**, 3065-3074 (2010).

55 Dromerick, A. W. & Reding, M. J. Functional Outcome for Patients With Hemiparesis, Hemihypesthesia, and Hemianopsia. *Stroke* **26**, 2023-2026 (1995).

56 Cordes, D. *et al.* Mapping functionally related regions of brain with functional connectivity MRI (fcMRI). *Am J Neuroradiol* **21**, 1636-1644 (2000).

57 Solodkin, A., Hlustik, P., Chen, E. E. & Small, S. L. Fine modulation in network activation during motor execution and motor imagery. *Cereb Cortex* **14**, 1246-1255 (2004).

58 Grefkes, C., Eickhoff, S. B., Nowak, D. A., Dafotakis, M. & Fink, G. R. Dynamic intra- and interhemispheric interactions during unilateral and bilateral hand movements assessed with fMRI and DCM. *Neuroimage* **41**, 1382-1394 (2008).

59 Kasess, C. H. *et al.* The suppressive influence of SMA on M1 in motor imagery revealed by fMRI and dynamic causal modeling. *Neuroimage* **40**, 828-837 (2008).

60 Jiang, T., He, Y., Zang, Y. & Weng, X. Modulation of functional connectivity during the resting state and the motor task. *Hum Brain Mapp* **22**, 63-71 (2004).

61 Jeannerod, M. & Frak, V. Mental imaging of motor activity in humans. *Curr Opin Neurobiol* **9**, 735-739 (1999).

62 Gerardin, E. *et al.* Partially Overlapping Neural Networks for Real and Imagined Hand Movements. *Cereb Cortex* **10**, 1093-1104 (2000).

63 Berg, F. E., Swinnen, S. P. & Wenderoth, N. Hemispheric Asymmetries of the Premotor Cortex are Task Specific as Revealed by Disruptive TMS During Bimanual Versus Unimanual Movements. *Cereb Cortex* **20**, 2842-2851 (2010).

64 Schell, G. R. & Strick, P. L. The origin of thalamic inputs to the arcuate premotor and supplementary motor areas. *J Neurosci* **4**, 539-560 (1984).

65 Deecke, L. Bereitschaftspotential as an indicator of movement preparation in supplementary motor area and motor cortex. *Ciba F Symp* **132**, 231-250 (1987).

66 Rouiller, E. M. *et al.* Transcallosal connections of the distal forelimb representations of the primary and supplementary motor cortical areas in macaque monkeys. *Exp Brain Res* **102**, 227-243 (1994).

67 Wu, T. *et al.* Functional Connectivity of Cortical Motor Areas in the Resting State in Parkinson's Disease. *Hum Brain Mapp* **32**, 1443-1457 (2011).

68 Cordes, D. *et al.* Frequencies contributing to functional connectivity in the cerebral cortex in "resting-state" data. *Am J Neuroradiol* **22**, 1326-1333 (2001).

69 Buzsáki, G. & Draguhn, A. Neuronal oscillations in cortical networks. *Science* **304**, 1926-1929 (2004).

70 De Luca, M., Beckmann, C. F., De Stefano, N., Matthews, P. M. & Smith, S. M. fMRI resting state networks define distinct modes of long-distance interactions in the human brain. *Neuroimage* **29**, 1359-1367, doi:10.1016/j.neuroimage.2005.08.035 (2006).

71 Razavi, M. *et al.* Source of low-frequency fluctuations in functional MRI signal. *J Magn Reson Im* **27**, 891-897, doi:10.1002/jmri.21283 (2008).

72 Balduzzi, D., Riedner, B. A. & Tononi, G. A BOLD window into brain waves. *Proc Natl Acad Sci U S A* **105**, 15641-15642, doi:10.1073/pnas.0808310105 (2008).

73 Keilholz, S. D., Magnuson, M. & Thompson, G. Evaluation of data-driven network analysis approaches for functional connectivity MRI. *Brain Struct Funct* **215**, 129-140 (2010).

74 Arieli, A., Sterkin, A., Grinvald, A. & Aertsen, A. Dynamics of Ongoing Activity: Explanation of the Large Variability in Evoked Cortical Responses. *Science* **273**, 1868-1871 (1996).

75 Palva, J. M. & Palva, S. Infra-slow fluctuations in electrophysiological recordings, blood-oxygenation-level-dependent signals, and psychophysical time series. *Neuroimage* **62**, 2201-2211 (2012).

76 Raichle, M. E. *et al.* A default mode of brain function. *Proc Natl Acad Sci U S A* **98**, 676-682 (2001).

77 Buckner, R. L., Andrews-Hanna, J. R. & Schacter, D. L. The brain's default network: anatomy, function, and relevance to disease. *Ann NY Acad Sci* **1124**, 1-38 (2008).

78 Fox, M. D. & Greicius, M. Clinical applications of resting state functional connectivity. *Front Syst Neurosci* **4** (2010).

79 Gillebert, C. R. & Mantini, D. Functional connectivity in the normal and injured brain. *Neuroscientist* **19**, 509-522 (2013).

80 Geweke, J. Measurement of linear dependence and feedback between multiple time series. *J Am Statist Assoc* **77**, 304-313 (1982).

81 Dhamala, M., Rangarajan, G. & Ding, M. Analyzing information flow in brain networks with nonparametric Granger causality. *Neuroimage* **41**, 354-362, doi:10.1016/j.neuroimage.2008.02.020 (2008).

82 Uswatte, G., Taub, E., Morris, D., Light, K. & Thompson, P. A. The Motor Activity Log-28: assessing daily use of the hemiparetic armafter stroke. *Neurology* **67**, 1189-1194 (2006).

83 Folstein, M. F., Folstein, S. E. & McHugh, P. R. “Mini-mental state”: a practical method for grading the cognitive state of patients for the clinician. *J Psychiat Res* **12**, 189-198 (1975).

84 Fugl-Meyer, A. R., Jaasko, L., Leyman, I., Olsson, S. & Steglind, S. The post-stroke hemiplegic patient. 1. A method for evaluation of physical performance. *Scand J Rehabil Med* **7**, 13-31 (1975).

85 Talairach, J. & Tournoux, P. Co-planar Stereotaxic Atlas of the Human Brain. *Thieme Medical, New York* (1988).

86 Ashburner, J. & Friston, K. J. Nonlinear Spatial Normalization Using Basis Functions. *Hum Brain Mapp* **7**, 254-266 (1999).

87 Hayasaka, S. & Nichols, T. E. Combining voxel intensity and cluster extent with permutation test framework. *Neuroimage* **23**, 54-63 (2004).

88 Cordes, D. *et al.* Frequencies contributing to functional connectivity in the cerebral cortex in "resting-state" data. *Am J Neuroradiol* **22**, 1326-1333 (2001).

89 Lowe, M. J., Mock, B. J. & Sorenson, J. A. Functional connectivity in single and multislice echoplanar imaging using resting state fluctuations. *Neuroimage* **7**, 119-132 (1998).

90 Raichle, M. E. & Mintun, M. A. Brain Work and Brain Imaging. *Annu Rev Neurosci* **29**, 449-476 (2006).

91 Tuladhar, A. M. *et al.* Default Mode Network Connectivity in Stroke Patients. *PloS One* **8** (2013).

92 Tsai, Y. H. *et al.* Disruption of brain connectivity in acute stroke patients with early impairment in consciousness. *Front Psychol* **4** (2014).

93 Wang, L. *et al.* Amplitude of low-frequency oscillations in first-episode, treatment-naive patients with major depressive disorder: a resting-state functional MRI study. *PloS One* **7** (2012).

94 Otten, M. L. *et al.* Motor deficits correlate with resting state motor network connectivity in patients with brain tumours. *Brain* **135**, 1017-1026 (2012).

95 Wu, C. W. *et al.* Frequency specificity of functional connectivity in brain networks. *Neuroimage* **42**, 1047-1055, doi:10.1016/j.neuroimage.2008.05.035 (2008).

96 Rehme, A. K., Eickhoff, S. B., Wang, L. E., Fink, G. R. & Grefkes, C. Dynamic causal modeling of cortical activity from the acute to the chronic stage after stroke. *Neuroimage* **55**, 1147-1158, doi:10.1016/j.neuroimage.2011.01.014 (2011).

97 Grefkes, C. *et al.* Cortical connectivity after subcortical stroke assessed with functional magnetic resonance imaging. *Ann Neurol* **63**, 236-246, doi:10.1002/ana.21228 (2008).

98 Inman, C. S. *et al.* Altered resting-state effective connectivity of fronto-parietal motor control systems on the primary motor network following stroke. *Neuroimage* **59**, 227-237, doi:10.1016/j.neuroimage.2011.07.083 (2012).

99 Rowe, J. *et al.* Attention to action in Parkinson's disease: impaired effective connectivity among frontal cortical regions. *Brain* **125**, 276-289 (2002).

100 Jones, T. A. & Schallert, T. Use-dependent growth of pyramidal neurons after neocortical damage. *J Neurosci* **14**, 2140-2152 (1994).

101 Dum, R. P. & Strick, P. L. Motor areas in the frontal lobe of the primate. *Physiol Behav* **77**, 677-682 (2002).

102 Aizawa, H., Inase, M., Mushiake, H., Shima, K. & Tanji, J. Reorganization of activity in the supplementary motor area associated with motor learning and functional recovery. *Exp Brain Res* **84**, 668-671 (1991).

103 Lotze, M. *et al.* Activation of cortical and cerebellar motor areas during executed and imagined hand movements: an fMRI study. *J Cognitive Neurosci* **11**, 491-501 (1999).

104 Cerritelli, B., Maruff, P., Wilson, P. & Currie, J. The effect of an external load on the force and timing components of mentally represented actions. *Behav Brain Res* **108**, 91-96 (2000).

105 Kohl, R. M. & Fisicaro, S. A. Imaging goal-directed movement. *Res Q Exercise Sport* **66**, 17-31 (1995).

106 Dickstein, R. & Deutsch, J. E. Motor Imagery in Physical Therapist Practice. *Phys Ther* **87**, 942-953 (2007).

107 Jackson, P. L., Lafleur, M. F., Malouin, F., Richards, C. L. & Doyon, J. Functional cerebral reorganization following motor sequence learning through mental practice with motor imagery. *Neuroimage* **20**, 1171-1180 (2003).

108 Dancause, N. *et al.* Extensive cortical rewiring after brain injury. *J Neurosci* **25** (2005).

109 Page, S. J., Levine, P., Sisto, S. & Johnston, M. V. A randomized efficacy and feasibility study of imagery in acute stroke. *Clin Rehabil* **15**, 233-240 (2001).

110 Confalonieri, L. *et al.* Brain Activation in Primary Motor and Somatosensory Cortices during Motor Imagery Correlates with Motor Imagery Ability in Stroke Patients. *ISRN Neuro* **2012**, 1-17, doi:10.5402/2012/613595 (2012).

111 Jeannerod, M. *Motor Cognition: What Actions Tell the Self*. (Oxford University Press, 2006).

112 Yue, G. & Cole, K. J. Strength increases from the motor program: comparison of training with maximal voluntary and imagined muscle contractions. *J Neurophysiol* **67**, 1114-1123 (1992).

113 Page, S. J., Levine, P. & Leonard, A. Mental practice in chronic stroke: results of a randomized, placebo-controlled trial. *Stroke* **38**, 1293-1297 (2007).

114 Kosslyn, S. M., Margolis, J. A., Barrett, A. M., Goldknopf, E. J. & Daly, P. F. Age differences in imagery abilities. *Child Dev* **61**, 995-1010 (1990).

115 Kosslyn, S. M., Brunn, J., Cave, K. R. & Wallach, R. W. Individual differences in mental imagery ability: A computational analysis. *Cognition* **18**, 195-243 (1984).

116 Schuster, C., Glässel, A., Scheidhauer, A., Ettlin, T. & Butler, J. Motor Imagery Experiences and Use: Asking Patients after Stroke Where, When, What, Why, and How They Use Imagery: A Qualitative Investigation. *Stroke Res Treat* **2012** (2012).

117 Lehéricy, S. *et al.* Motor execution and imagination networks in post-stroke dystonia. *Neuroreport* **15**, 1887-1890 (2004).

118 Mintzopoulos, D. *et al.* Connectivity alterations assessed by combining fMRI and MR-compatible hand robots in chronic stroke. *Neuroimage* **47**, T90-T97 (2009).

119 Jiang, L., Xu, H. & Yu, C. Brain Connectivity Plasticity in the Motor Network after Ischemic Stroke. *Neural Plast* **924192** (2013).

120 Friston, K., Moran, R. & Seth, A. K. Analysing connectivity with Granger causality and dynamic causal modelling. *Curr Opin Neurobiol* **23**, 1-7 (2012).

121 Hale, B. D. The Effects of Internal and External Imagery on Muscular and Ocular Concomitants. *J Sport Psychol* **4**, 379-387 (1982).

122 Livesay, J. R. & Samaras, M. R. Covert neuromuscular activity of the dominant forearm during visualization of a motor task. *Percept Mot Skills* **86**, 371-374 (1998).

123 Altschuler, E. L. *et al.* Rehabilitation of hemiparesis after stroke with a mirror. *Lancet* **353**, 2035-2036 (1999).

124 Silasi, G. & Murphy, T. H. Stroke and the Connectome: How Connectivity Guides Therapeutic Intervention. *Neuron* **83**, 1354-1368 (2014).

125 Grefkes, C. & Fink, G. R. Connectivity-based approaches in stroke and recovery of function. *Lancet Neurol* **13**, 206-216 (2014).

126 Schaechter, J. D. *et al.* Motor recovery and cortical reorganization after constraint-induced movement therapy in stroke patients: a preliminary study. *Neurorehab Neural Re* **16**, 326-338 (2002).

127 Wittenberg, G. *et al.* Constraint-induced therapy in stroke: magnetic-stimulation motor maps and cerebral activation. *Neurorehab Neural Re* **17**, 48-57 (2003).

128 Jeannerod, M. Mental imagery in the motor context. *Neuropsychologia* **33**, 1419-1432 (1995).

129 Walsh, R. R., Small, S. L., Chen, E. E. & Solodkin, A. Network activation during bimanual movements in humans. *Neuroimage* **43**, 540-553, doi:10.1016/j.neuroimage.2008.07.019 (2008).

130 Rehme, A. K., Eickhoff, S. B. & Grefkes, C. State-dependent differences between functional and effective connectivity of the human cortical motor system. *Neuroimage* **67**, 237-246, doi:10.1016/j.neuroimage.2012.11.027 (2013).

131 Gao, Q., Duan, X. & Chen, H. Evaluation of effective connectivity of motor areas during motor imagery and execution using conditional Granger causality. *Neuroimage* **54**, 1280-1288, doi:10.1016/j.neuroimage.2010.08.071 (2011).

132 Gregg, M., Hall, C. & Butler, A. The MIQ-RS: A Suitable Option for Examining Movement Imagery Ability. *Evid Based Complement Alternat Med* **7**, 249-257 (2010).

133 Butler, A. J. *et al.* The Movement Imagery Questionnaire-Revised, Second Edition (MIQ-RS) Is a Reliable and Valid Tool for Evaluating Motor Imagery in Stroke Populations. *Evid Based Complement Alternat Med* **2012**, doi:10.1155/2012/497289 (2012).

134 Mazziotta, J. C., Toga, A. W., Evans, A., Fox, P. & Lancaster, J. A Probablistic Atlas of the Human Brain: Theory and Rationale for Its Development. *Neuroimage* **2**, 89-101 (1995).

135 Jones, O. P. *et al.* Auditory–Motor Interactions for the Production of Native and Non-Native Speech. *J Neurosci* **33**, 2376-2387 (2013).

136 Li, J. *et al.* Effective connectivities of cortical regions for top-down face processing: a dynamic causal modeling study. *Brain Res* **1340**, 40-51, doi:10.1016/j.brainres.2010.04.044 (2010).

137 Bajaj, S., Lamichhane, B., Adhikari, B. M. & Dhamala, M. Amygdala Mediated Connectivity in Perceptual Decision-Making of Emotional Facial Expressions. *Brain Conn* **3**, 386-397 (2013).

138 Boussaoud, D., Tanné-Gariépy, J., Wannier, T. & Rouiller, E. Callosal connections of dorsal versus ventral premotor areas in the macaque monkey: a multiple retrograde tracing study. *BMC Neurosci* **6** (2005).

139 Luppino, G., Matelli, M., Camarda, R. & Rizzolatti, G. Corticocortical connections of area F3 (SMA-proper) and area F6 (pre-SMA) in the macaque monkey. *J Comp Neurol* **338**, 114-140 (1993).

140 Dima, D., Stephan, K. E., Roiser, J. P., Friston, K. J. & Frangou, S. Effective connectivity during processing of facial affect: evidence for multiple parallel pathways. *J Neurosci* **31**, 14378-14385, doi:10.1523/JNEUROSCI.2400-11.2011 (2011).

141 Raffin, E., Mattout, J., Reilly, K. T. & Giraux, P. Disentangling motor execution from motor imagery with the phantom limb. *Brain* **135**, 582-595 (2012).

142 Xu, L. *et al.* in *Medical Imaging 2013: Biomedical Applications in Molecular, Structural, and Functional Imaging* Vol. 8672 (Orlando, Florida, United States, 2013).

143 Westlake, K. P. & Nagarajan, S. S. Functional connectivity in relation to motor performance and recovery after stroke. *Front Syst Neurosci* **5**, 8, doi:10.3389/fnsys.2011.00008 (2011).

144 Hanakawa, T., Dimyan, M. A. & Hallett, M. Motor planning, imagery, and execution in the distributed motor network: a time-course study with functional MRI. *Cereb Cortex* **18**, 2775-2788 (2008).

145 Munzert, J., Lorey, B. & Zentgraf, K. Cognitive motor processes: the role of motor imagery in the study of motor representations. *Brain Res Rev* **60**, 306-326 (2009).

146 Li, S., Kamper, D. G., Stevens, J. A. & Rymer, W. Z. The effect of motor imagery on spinal segmental excitability. *J Neurosci* **24**, 9674-9680 (2004).

147 Brown, C. E., Aminoltejari, K., Erb, H., Winship, I. R. & Murphy, T. H. In Vivo Voltage-Sensitive Dye Imaging in Adult Mice Reveals That Somatosensory Maps Lost to Stroke Are Replaced over Weeks by New Structural and Functional Circuits with Prolonged Modes of Activation within Both the Peri-Infarct Zone and Distant Sites. *J Neurosci* **29**, 1719-1734 (2009).

148 Mostany, R. *et al.* Local hemodynamics dictate long-term dendritic plasticity in peri-infarct cortex. *J Neurosci* **30**, 14116-14126 (2010).

149 Nudo, R. J., Milliken, G. W., Jenkins, W. M. & Merzenich, M. M. Use-dependent alterations of movement representations in primary motor cortex of adult squirrel monkeys. *J Neurosci* **16**, 785-807 (1996).

150 Arya, K. N., Pandian, S., Verma, R. & Garg, R. K. Movement therapy induced neural reorganization and motor recovery in stroke: A review. *J Bodyw Mov Ther* **15**, 528-537 (2011).

151 Krakauer, J. W. Motor learning: its relevance to stroke recovery and neurorehabilitation. *Curr Opin Neurobiol* **19**, 84-90 (2006).

152 Davis, J. Z. Task selection and enriched environments: a functional upper extremity training program for stroke survivors. *Top Stroke Rehabil* **13**, 1-11 (2006).

153 Nudo, R. J., Friel, K. M. & Delia, S. W. Role of sensory deficits in motor impairments after injury to primary motor cortex. *Neuropharmacol* **39**, 733-742 (2000).

APPENDICES

Appendix A

Power and Granger causality (GC) spectra are shown below for five regions of interest (ROIs): the left primary motor area (LM1), the right primary motor area (RM1), the left premotor cortex (LPMC), the right premotor cortex (RPMC) and the supplementary motor area (SMA) for young able-bodied (AB), aged stroke-survivors (SS) following stroke, aged stroke survivors following mental practice (MP) only and following combined treatment of mental practice and physical therapy (MP+PT).

A.1: Power spectra for young able-bodied and aged stroke-survivors

For all five ROIs: LM1, RM1, LPMC, RPMC and SMA, average power spectra were computed from all subjects for (A) AB, (B) SS, (C) MP and (D) MP+PT conditions. Peak of power spectra for all the ROIs under all the conditions was found in the frequency range 0.06-0.08 Hz.

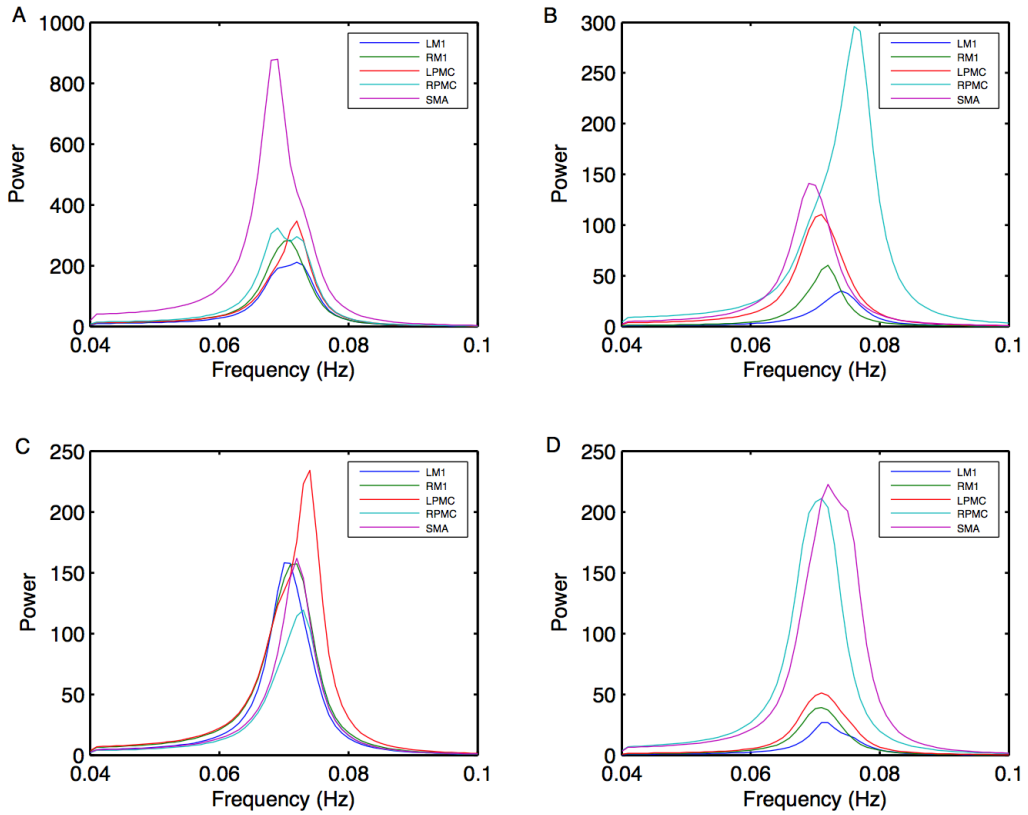

A.2: Granger causality spectra for young able-bodied and aged stroke-survivors

Granger causality (GC) spectra for all the possible connections among five ROIs (LM1, RM1, LPMC, RPMC and SMA) were computed. Seven connections (A-G) were found which were significantly stronger for AB condition (blue colored plots) whereas none of the connections was significantly stronger for aged stroke survivors following stroke (black colored plots) as well as following MP (red colored plots). Three connections (A, D and F) were significantly stronger for participants who underwent MP+PT (green colored plots).

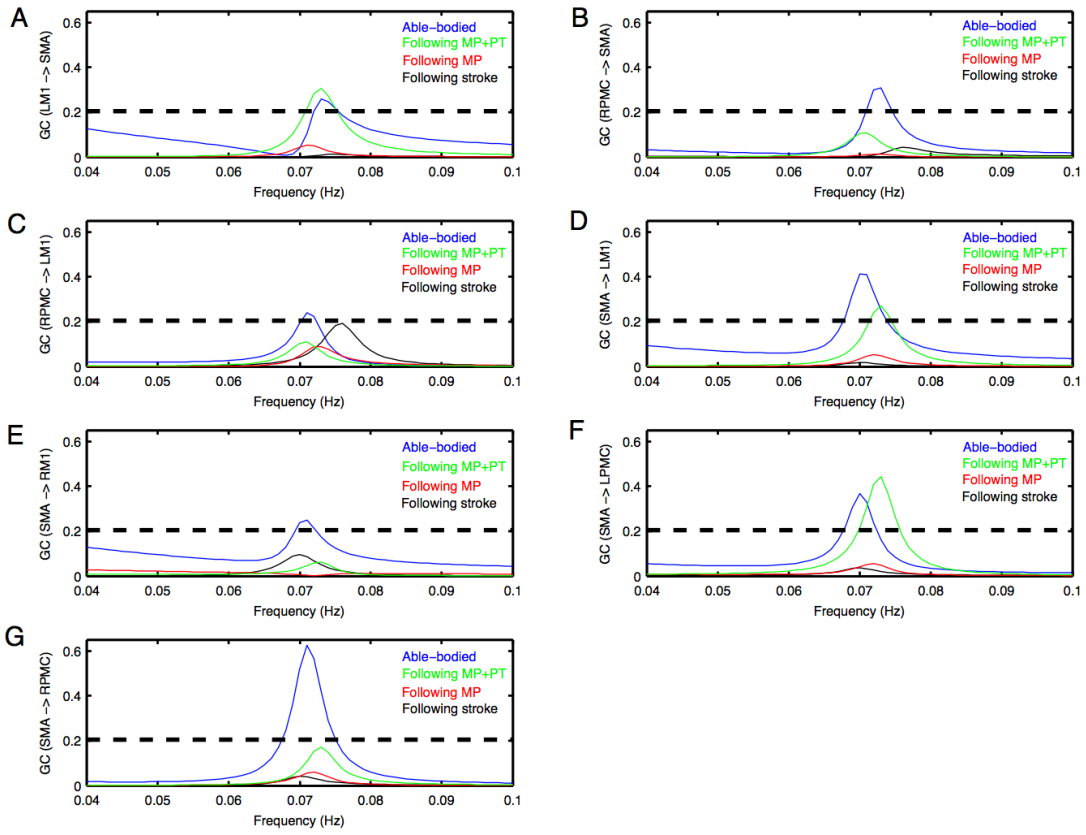

Dashed lines in the GC plots show a significant threshold ($p < 0.01$, sample size = 26) calculated from combined set of data for AB and SS. Peak of GC spectra for all the ROIs under all the conditions was also found in the same frequency range 0.06-0.08 Hz.